Mathematical Biosciences and Engineering

http://www.aimspress.com/journal/mbe

MBE, 23(5): 1501–1533.
DOI: 10.3934/mbe.2026055
Received: 27 January 2026
Revised: 19 March 2026
Accepted: 07 April 2026
Published: 16 April 2026

Research article

Modeling the impact of budget limitation on the screening and treatment pathway of HPV-induced precancerous cervical lesions

Marius Tadjuidje Fodjo[1], Aurelien Kambeu Youmbi[1], Maison Mayeh[2,3], Solange Whegang[4], Bruno Kenfack[4] and Berge Tsanou[1,5,*]

[1] Department of Mathematics and Computer Science, University of Dschang, Dschang, Cameroon
[2] Ministry of Public Health, Douala General Hospital, Radiology-Oncology Department, Cameroon
[3] Faculty of Medicine and Pharmaceutical Sciences, University of Douala, Douala, Cameroon
[4] Faculty of Medicine and Pharmaceutical Sciences, University of Dschang, Dschang, Cameroon
[5] Department of Mathematics and Applied Mathematics, University of Pretoria, South Africa

* **Correspondence:** Email: bergetsanou@gmail.com.

Abstract: Cervical cancer in women remains a major public health challenge in sub-Saharan Africa, where both the late diagnoses and limited financial resources hinder effective prevention and treatment. We propose an economic–epidemiological model that integrates the care pathway for cervical lesions and the financial ability to access different treatment stages. Analytical results establish the existence of a basic economic threshold $\mathcal{R}_0$, whose value determines whether the system sustains preventive care or collapses into diagnostic failure. We show that a backward bifurcation can occur when $\mathcal{R}_0 < 1$, leading to the coexistence of two stable equilibrium points. Furthermore, we establish the global stability of the system collapse equilibrium when $\mathcal{R}_0 \leq 1$ under specific conditions. Sensitivity analysis identifies key economic parameters such as screening subsidy, treatment cost, and patient contribution to the billing account that critically influence model dynamics. Numerical simulations estimate that a minimum subsidy level of approximately 13.1% of the human papillomavirus (HPV) test cost is required to ensure system viability ($\mathcal{R}_0 > 1$) and prevent long-term collapse of screening coverage. We further decompose the total treatment cost across the care stages and formulate an optimization problem to determine the optimal allocation of government subsidies, minimizing treatment costs while ensuring 90% coverage of women who test positive for HPV. The results show that the optimal strategy requires the government to cover 21.65% of the total treatment cost, mainly focusing on the eligibility test and Large loop excision of the transformation zone (LLETZ) treatment. These findings highlight the importance of targeted subsidies to guarantee both accessibility and financial sustainability in the treatment of precancerous cervical lesions.

Keywords: precancerous cervical lesions; care pathway; government subsidy; modeling; optimization

1. Introduction

Cervical cancer remains one of the most common malignancies affecting women worldwide [1, 2]. It develops from untreated precancerous lesions caused by persistent infection with high-risk types of human papillomavirus (HPV). According to [3], about 94% of cervical cancer deaths occur in low- and middle-income countries, with sub-Saharan Africa bearing the highest burden. In Cameroon, despite awareness campaigns and free screening initiatives, morbidity and mortality rates remain high [4].

Screening, mainly through the HPV test, is the most effective preventive strategy. If a woman tests positive, she undergoes an eligibility test for ablative treatment. When lesions are not suitable for ablation, more advanced procedures such as large loop excision of the transformation zone (LLETZ) or biopsy are recommended. However, access to screening and treatment remains a major challenge. Each step of the pathway (HPV test, eligibility test, treatment, and biopsy) involves direct costs that are often paid by the patients themselves. As a result, participation in screening programs remains low. This is further aggravated by the fact that cervical cancer is often asymptomatic in its early stages, leading many women to underestimate its risks. Misinformation, out-of-pocket expenses, and fragmented care pathways therefore reduce the effectiveness of current prevention strategies [5]. Recent advances in medical research, computational modeling, and artificial intelligence have improved the detection and characterization of precancerous cervical lesions, notably through AI-assisted diagnostic and image analysis systems [6]. However, in many low- and middle-income countries, the main challenge remains the accessibility and continuity of care along the screening and treatment pathway, where financial barriers often limit the population-level impact of these technological advances.

In the Cameroonian context, recent studies have highlighted critical gaps in both clinical access and financing. [5] quantified the actual cost of cervical cancer treatment through radiotherapy, revealing significant out-of-pocket burden for patients. [7] analyzed the clinical and epidemiological characteristics of cervical cancer cases in Douala, confirming the predominance of advanced-stage diagnoses. In parallel, [8] showed that insufficient knowledge and preventive practices among health professionals contribute to low screening coverage.

Existing mathematical models of cervical cancer screening and treatment have contributed significantly to our understanding of disease dynamics (see [9–11] and references therein). However, none of these models or studies explicitly analyze how financial constraints affect the entire care pathway. Thus, there is a critical need to investigate models that couple epidemiological processes with financial accessibility mechanisms (see [12] and references therein).

This study develops and analyzes an economic–epidemiological model for the screening and treatment pathway of precancerous cervical lesions under financial constraints. The model incorporates both clinical transitions (screening, eligibility testing, LLETZ treatment, and biopsy) and the economic ability to access care. Its objective is to quantify the impact of financial barriers on screening coverage and treatment continuity, and to assess the potential benefits of targeted government subsidies. More specifically, we determine the economic threshold governing system sustainability, identify the key financial parameters affecting viability, and propose optimized subsidy strategies to improve access to care.

We establish the existence of a basic economic threshold $\mathcal{R}_0$, whose value determines whether the system sustains preventive care or collapses into diagnostic failure. We show that a backward bifurcation can occur when $\mathcal{R}_0 < 1$, leading to the coexistence of multiple stable equilibrium points.

Furthermore, we establish the global stability of the collapse system equilibrium when $\mathcal{R}_0 < 1$ under specific conditions. Sensitivity analysis via partial rank correlation coefficient (PRCC) and extended Fourier amplitude sensitivity test (eFAST) identifies key economic parameters such as screening subsidy, treatment cost, and patient contribution to the billing account that critically influence model dynamics. Numerical simulations estimate that a minimum subsidy level of approximately 13.1% of the HPV test cost is required to ensure system viability ($\mathcal{R}_0 \geq 1$) and prevent long-term collapse of screening coverage. We further decompose the total treatment cost across the care stages and formulate an optimization problem to determine the optimal allocation of government subsidies, minimizing treatment costs while ensuring 90% coverage of women who test positive for HPV. The results show that the optimal strategy requires the government to cover 21.65% of the total treatment cost, focusing mainly on the eligibility test and LLETZ treatment.

The paper is organized as follows. Section 2 provides a detailed description of the cervical cancer care pathway in Cameroon, highlighting the clinical steps under financial constraints, and presents the model formulation. Section 3 discusses the mathematical analysis, including equilibrium points, their stability, and bifurcation analysis. In Section 4 we discuss parameter estimation. In Section 5 we report the sensitivity analysis using PRCC and eFAST methods to identify key parameters that influence the outcomes of the model. Section 6 evaluates the total cost of care over a 10-year horizon, formulates and interprets a subsidy allocation optimization problem under constraints $\mathcal{R}_0 > 1$. Finally, the conclusion is drawn in Section 7.

2. Modeling framework

2.1. Description of the care pathway for cervical cancer screening

According to oncologists operating in various treatment centers, including Dschang Regional Hospital, the cervical cancer care pathway they follow is based on the World Health Organization (WHO) algorithm [13], and is composed of sequential clinical stages, each with its own access barriers, mainly economic. The process typically begins with a screening phase, often using the HPV test to detect high-risk types of HPV. Women who test negative are generally advised to repeat the test after five years, as the risk of progression of the lesions remains low [14].

For women who test positive, a second diagnostic step is performed: a visual inspection with acetic acid (VIA), also called the eligibility test for ablative treatment. This test assesses whether lesions are localized and suitable for immediate treatment using thermal ablation. When the lesions are not eligible due to dispersion, location, or severity further diagnostic or therapeutic interventions are required. When the lesions are localized, women may receive thermal ablation, a low-cost outpatient procedure that uses a heated probe to destroy precancerous cells. When ablation is not feasible, for instance due to lesion dispersion or anatomical considerations, the recommended alternative is the large loop excision of the transformation zone (LLETZ), a more advanced procedure that requires electricity and trained personnel. Finally, when malignant transformation is suspected or treatment outcomes remain uncertain, a biopsy is performed to confirm the diagnosis and mark the transition to invasive cancer management. Access to each procedure directly determines whether patients can continue along the care pathway. Economic constraints are a major cause of dropout at every stage, especially between diagnosis and treatment. In this study, economic constraints refer to barriers that limit women's access to care, including the relatively low minimum wage in Cameroon (around 43,969 XAF/month [15]), the high cost of living

in urban areas, and the widespread reliance on out-of-pocket payments. For example, local clinical data reported a unit price of 30,000 XAF for a biopsy. The cumulative burden of direct medical costs, combined with indirect costs (e.g., transport, time lost), leads many women to forgo care even after a positive diagnosis.

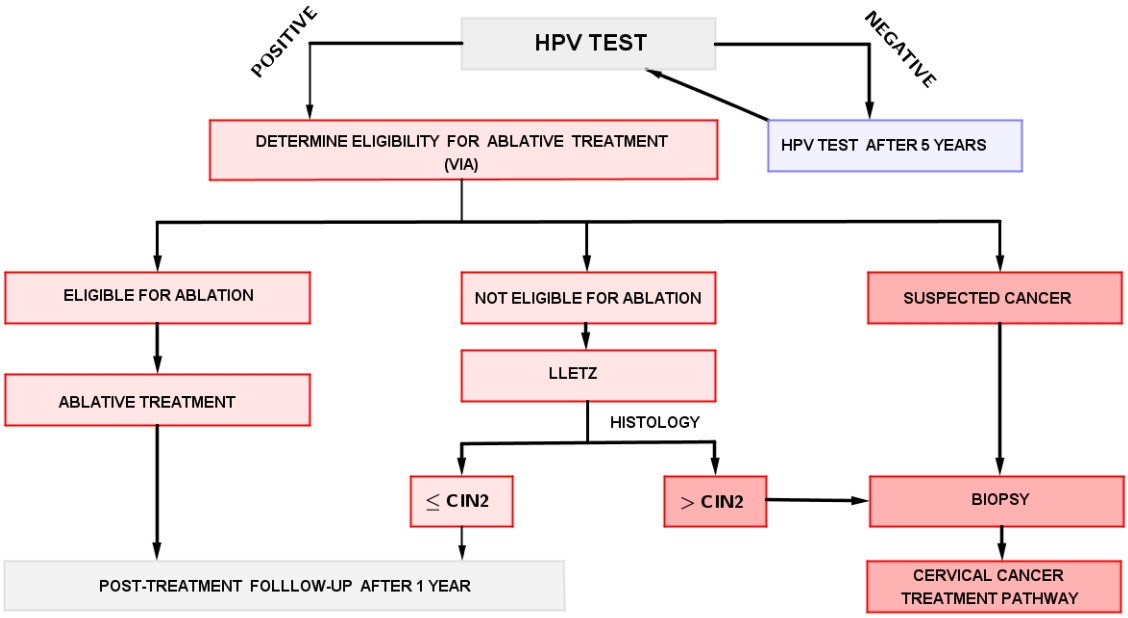

Figure 1. Schematic representation of the care pathway for primary HPV DNA test screening for general population of women. The figure highlights the main steps of the process, from the initial HPV test to eligibility testing and treatment options. This is an adaptation of the algorithm proposed by the World Health Organization [13]. CIN2 stands for cervical intraepithelial neaoplasia grade 2.

2.2. *From care pathway to model variables*

To bridge the clinical care pathway of Figure 1 with the mathematical model, we adopt a compartmental modeling approach using ordinary differential equations. We first define the state variables that represent the main compartments of the system. The goal is to describe the main steps of cervical cancer screening in a simplified way, so that the care process is easy to follow and can still be analyzed with mathematical tools.

The screened population, denoted by S_T, corresponds to women who received the HPV test. The entry into this compartment marks the beginning of the involvement in the preventive program, and the exit depends on the test results and subsequent referral to further diagnostic steps. Women who are tested positive move to the eligibility test for the ablative treatment stage (T_A), where examinations such as visual inspection after acetic acid application (VIA) or ventilator-induced lung injury (VILI) are used to check if they can safely receive ablative treatment. Women considered eligible for thermal ablation are assigned to compartment E_1, representing the group of patients who undergo ablative treatment. Successful outcomes may lead to a return to screening. Those who are not eligible for ablation are referred to the LLETZ treatment stage E_2. As in the case of ablation, successfully treated patients

can also result in re-entry into the screening compartment S_T. The compartment B represents women who undergo biopsy, whether due to failure in treatment, diagnostic uncertainty, or direct referral to eligibility testing.

Beyond the clinical compartments, we introduce a financial variable M to represent the amount available to support screening and treatment. This variable is central to the model because access to care depends not only on clinical eligibility but also on the availability of sufficient funds. It increases through out-of-pocket contributions and decreases as costs are paid at each stage of care. Several transition rates are therefore linked to M, meaning that movement from one stage to the next depends directly on financial resources. By coupling the clinical pathway with this financial constraint, the model captures both the medical process and the economic barriers that can limit the sustainable functioning of the healthcare system.

2.3. Dynamics equations of the care pathway

Exploiting the clinical transitions in the screening pathway described in Figure 1 and the influence of the patient's billing account M during these transitions, the dynamics of the screening care pathway is modeled by a system of deterministic ordinary differential equations (ODEs).

Women first access screening through HPV testing. The inflow into the screened class S_T follows a Holling type II functional response [16], expressed as $\Lambda_1 M/(\delta + M)$. Women may re-enter this compartment after successful treatment through either ablation or LLETZ at rates $\gamma_1 M$ and $\gamma_2 M$, respectively. They exit screening to receive eligibility test ($\alpha_T M$) when the test is positive, or after five years at the rate μ_S if the test is negative. Therefore, the dynamic of S_T is given by

$$\frac{\mathrm{d}S_T}{\mathrm{d}t} = \frac{\Lambda_1 M}{\delta + M} + \gamma_1 M E_1 + \gamma_2 M E_2 - \alpha_T M S_T - \mu_S S_T. \tag{2.1}$$

Women who are tested positive, denoted by T_A, may proceed to the eligibility test, provided they can afford its cost p_T. This compartment also receives women whose ablative treatment fails, at rate ηM. Individuals leave T_A to receive ablation, LLETZ, or biopsy, with rates $\lambda_1 M$, $\lambda_2 M$, and $\lambda_3 M$, respectively. In addition, a fraction exit this stage at rate μ_T, representing women who discontinue the care process. The corresponding equation is

$$\frac{\mathrm{d}T_A}{\mathrm{d}t} = \alpha_T M S_T + \eta M E_1 - (\lambda_1 + \lambda_2 + \lambda_3) M T_A - \mu_T T_A. \tag{2.2}$$

From the eligibility stage, some women receive thermal ablation, denoted by E_1. Their inflow occurs at the rate $\lambda_1 M$. Within this compartment, treatment may succeed, returning women to S_T at rate $\gamma_1 M$, or fail, returning them to T_A at rate ηM. Women may also exit the system at the rate μ_1, due to reasons such as abandonment or loss to follow-up. Thus, the dynamic of E_1 is

$$\frac{\mathrm{d}E_1}{\mathrm{d}t} = \lambda_1 M T_A - \gamma_1 M E_1 - \eta M E_1 - \mu_1 E_1. \tag{2.3}$$

Another fraction of women receive LLETZ treatment, denoted by E_2, with inflow rate $\lambda_2 M$. They may return to screening after successful treatment at rate $\gamma_2 M$ or be referred to biopsy in the case of failure at rate βM. Women may also exit the system at the rate μ_2 due to reasons such as abandonment or loss to follow-up. The governing equation is

$$\frac{\mathrm{d}E_2}{\mathrm{d}t} = \lambda_2 M T_A - \gamma_2 M E_2 - \beta M E_2 - \mu_2 E_2. \tag{2.4}$$

Women may also reach the biopsy stage B, either directly from eligibility testing with inflow rate $\lambda_3 M$ or following LLETZ failure (βM). This is the final stage of the modeled pathway, after which invasive cancer treatment begins. The exit rate of this compartment is μ_B. The dynamic is described by

$$\frac{\mathrm{d}B}{\mathrm{d}t} = \lambda_3 M T_A + \beta M E_2 - \mu_B B. \tag{2.5}$$

The previous descriptions are represented by Figure 2.

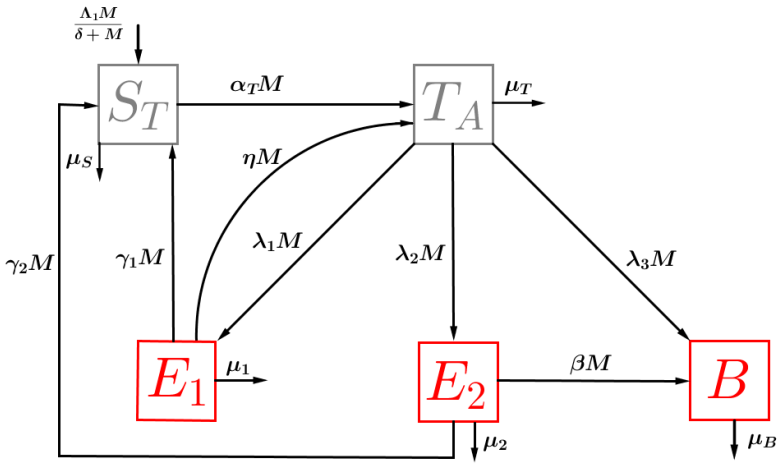

Figure 2. Simplified flow chart of model (2.7). The variables are: women screened for HPV (S_T), women who received VIA (T_A), women who received ablative treatment (E_1), women who received LLETZ treatment (E_2), women who underwent a biopsy (B). The dynamic of the patient billing account M is not represented here.

Table 1. State variables of model (2.7).

Variable	Description
S_T	Women screened for HPV
T_A	Women received VIA
E_1	Women received ablative treatment
E_2	Women received LLETZ treatment
B	Women underwent biopsy
M	Patient billing account

The patient billing account M evolves according to financial inflows and outflows. It is credited daily by the average patient's contribution qN, where $N = S_T + T_A + E_1 + E_2 + B$ is the total number of women within the care pathway. This formulation is consistent with healthcare financing systems largely based on out-of-pocket payments, where the total financial inflow increases proportionally with the number of patients receiving care [17]. It decreases through natural depletion $\mu_M M$, as well as payments for screening, diagnostic tests, treatments, and biopsies, each weighted by the corresponding subsidy rate; Each parameter ϵ_X represents the proportion of the medical cost paid by the patient for the procedure X. A value of $\epsilon_X = 1$ corresponds to the absence of a government subsidy (full out-of-pocket cost), while

$\epsilon_X = 0$ implies a full subsidy. Intermediate values $0 < \epsilon_X < 1$ represent partial subsidies. This leads to

$$\begin{aligned}\frac{\mathrm{d}M}{\mathrm{d}t} =& qN - \mu_M M - \epsilon_S p_S \left(\frac{\Lambda_1 M}{\delta + M} + \gamma_1 M E_1 + \gamma_2 M E_2\right) \\ & - \epsilon_T p_T \left(\alpha_T M S_T + \eta M E_1\right) - \epsilon_A p_A \lambda_1 M T_A - \epsilon_L p_L \lambda_2 M T_A \\ & - \epsilon_B p_B \left(\lambda_3 M T_A + \beta M E_2\right).\end{aligned} \tag{2.6}$$

Table 2. Description of the parameters of model (2.7).

Parameter	Description	Value	Units	Source
Λ_1	Daily inflow of women accessing screening	50	persons · day^{-1}	Estimated
δ	Half-saturation constant in screening rate	500	XAF	Estimated
α_T	Transition rate to eligibility test (per unit of currency)	4.12×10^{-5}	XAF^{-1}· day^{-1}	Estimated
p_S	Cost of HPV screening test	10,000	XAF · person^{-1}	[18]
$1 - \epsilon_S$	Proportion of state subsidy for HPV test	0	–	[Local Clinics]
p_T	Cost of eligibility test for ablative treatment	5000	XAF · person^{-1}	[18]
$1 - \epsilon_T$	Proportion of state subsidy for eligibility test	0	–	[Local Clinics]
p_A	Cost of ablative treatment	5000	XAF · person^{-1}	[Local Clinics]
$1 - \epsilon_A$	Proportion of state subsidy for ablative treatment	0	–	[Local Clinics]
p_L	Cost of LLETZ treatment	20,000	XAF · person^{-1}	[Local Clinics]
$1 - \epsilon_L$	Proportion of state subsidy for LLETZ treatment	0	–	[Local Clinics]
p_B	Cost of cervical biopsy	30,000	XAF · person^{-1}	[Local Clinics]
$1 - \epsilon_B$	Proportion of state subsidy for biopsy	0	–	[Local Clinics]
q	Daily patient contribution to billing account	4.8	XAF · day^{-1}	Estimated
λ_1	Transition rate to ablative treatment (per unit of currency)	1.25×10^{-4}	XAF^{-1}· day^{-1}	Estimated
λ_2	Transition rate to LLETZ treatment	1.25×10^{-5}	XAF^{-1}· day^{-1}	Estimated
λ_3	Transition rate to biopsy (direct from T_A)	4.16×10^{-6}	XAF^{-1}· day^{-1}	Estimated
η	Failure rate of ablative treatment	1.2×10^{-5}	XAF^{-1}· day^{-1}	Estimated
β	Transition rate to biopsy after LLETZ failure	4×10^{-6}	XAF^{-1}· day^{-1}	Estimated
γ_1	Return rate to screening after successful ablation	9.40×10^{-5}	XAF^{-1}· day^{-1}	Estimated
γ_2	Return rate to screening after successful LLETZ	8.80×10^{-5}	XAF^{-1}· day^{-1}	Estimated
μ_1, μ_2	Exit rates in ablatio compartment	4.15×10^{-5}	day^{-1}	Estimated
μ_S	Exit rate in screening compartment	5.47×10^{-4}	day^{-1}	Estimated
μ_B	Exit rate in biopsy compartment	0.1	day^{-1}	Estimated
μ_T	Exit rate in VIA compartment	1.0×10^{-5}	day^{-1}	Assumed
μ_M	Natural depletion rate on the billing account	4.1×10^{-4}	day^{-1}	Assumed

Combining the clinical transitions and the financial dynamics described above, we obtain the following nonlinear ODEs system:

$$\begin{cases} \dfrac{\mathrm{d}S_T}{\mathrm{d}t} = \dfrac{\Lambda_1 M}{\delta + M} + \gamma_1 M E_1 + \gamma_2 M E_2 - \alpha_T M S_T - \mu_S S_T, \\ \dfrac{\mathrm{d}T_A}{\mathrm{d}t} = \alpha_T M S_T + \eta M E_1 - (\lambda_1 + \lambda_2 + \lambda_3) M T_A - \mu_T T_A, \\ \dfrac{\mathrm{d}E_1}{\mathrm{d}t} = \lambda_1 M T_A - \gamma_1 M E_1 - \eta M E_1 - \mu_1 E_1, \\ \dfrac{\mathrm{d}E_2}{\mathrm{d}t} = \lambda_2 M T_A - \gamma_2 M E_2 - \beta M E_2 - \mu_2 E_2, \\ \dfrac{\mathrm{d}B}{\mathrm{d}t} = \lambda_3 M T_A + \beta M E_2 - \mu_B B, \\ \dfrac{\mathrm{d}M}{\mathrm{d}t} = qN - \mu_M M - \epsilon_S p_S \left(\dfrac{\Lambda_1 M}{\delta + M} + \gamma_1 M E_1 + \gamma_2 M E_2\right) - \epsilon_T p_T \left(\alpha_T M S_T + \eta M E_1\right), \\ \qquad - \epsilon_A p_A \lambda_1 M T_A - \epsilon_L p_L \lambda_2 M T_A - \epsilon_B p_B \left(\lambda_3 M T_A + \beta M E_2\right), \end{cases} \tag{2.7}$$

with the following initial conditions:

$$S_T(0) \geq 0,\ T_A(0) \geq 0,\ E_1(0) \geq 0,\ E_2(0) \geq 0,\ B(0) \geq 0,\ M(0) \geq 0. \tag{2.8}$$

A complete list of the state variables and the parameters including their numerical values and units, is provided in Tables 1 and 2, respectively.

3. Mathematical analysis

We analyze the well-posedness of the model and derive its equilibrium points and their stability conditions.

Since the vector field in system (2.7) is continuously differentiable (C^1), the Cauchy-Lipschitz theorem warrants the local existence and uniqueness of the solution of problem (2.7) and (2.8).

We now study the positivity and boundedness of this solution. The nonnegativity of each variable is ensured by analyzing the vector field on the boundary of the nonnegative orthant $\mathbb{R}^6_+$, following the method in [19]. We now show that all solutions remain bounded in the following theorem.

Theorem 1 (Invariant region)**.** *We set*

$$\Gamma := \left\{(S_T, T_A, E_1, E_2, B, M)^T \in \mathbb{R}^6_+ \ :\ N(t) \leq N_{\max},\ M(t) \leq M_{\max}\right\},$$

where $N(t) = S_T + T_A + E_1 + E_2 + B$, $N_{\max} = \max\{N_0, \Lambda_1/\mu\}$, *and* $M_{\max} = \max\{M_0,\ qN_{\max}/\mu_M\}$. *Then,* Γ *is positively invariant under the flow of system* (2.7).

Proof. Let $(S_T, T_A, E_1, E_2, B, M)^T \in \mathbb{R}^6_+$ be a maximal solution of (2.7) and (2.8), and $N(t) = S_T + T_A + E_1 + E_2 + B$. By summing the first five equations of system (2.7), one has

$$\dot{N} = \frac{\Lambda_1 M}{\delta + M} - \mu_S S_T - \mu_T T_A - \mu_1 E_1 - \mu_2 E_2 - \mu_B B.$$

Bounding all negative terms by μN, where $\mu = \min\{\mu_S, \mu_T, \mu_1, \mu_2, \mu_B\}$, gives

$$\dot{N} \leq \Lambda_1 - \mu N,$$

According to Gronwall's inequality, we get

$$N(t) \leq \left(N_0 - \frac{\Lambda_1}{\mu}\right) e^{-\mu t} + \frac{\Lambda_1}{\mu} \leq N_{\max}.$$

Similarly, from the equation of $\dot{M}$ in (2.7), we have

$$\dot{M}(t) \leq qN(t) - \mu_M M(t) \leq qN_{\max} - \mu_M M(t),$$

which gives

$$M(t) \leq \max\left\{M_0,\ \frac{qN_{\max}}{\mu_M}\right\} = M_{\max}.$$

Therefore, we have shown that $N(t) \leq N_{\max}$ and $M(t) \leq M_{\max}$ for all $t \geq 0$. Since all state variables remain nonnegative and bounded by the definitions of $N_{\max}$ and $M_{\max}$, the region Γ is positively invariant under the flow of system (2.7). This completes the proof.

3.1. Asymptotic behavior

To determine the equilibrium points of system (2.7), we set the derivatives equal to zero. The collapse equilibrium corresponds to the case where the patient's billing account is empty, i.e., $M = 0$. Solving the system with $M = 0$, we obtain:

$$E_0 = (S_T, T_A, E_1, E_2, B, M) = (0, 0, 0, 0, 0, 0).$$

The local stability of E_0 is studied by linear stability analysis, based on the Jacobian matrix evaluated at this equilibrium.

Indeed, the Jacobian matrix J of the system (2.7), with respect to variables $(S_T, T_A, E_1, E_2, B, M)$, is evaluated in E_0 as follows:

$$J(E_0) = \begin{bmatrix} -\mu_S & 0 & 0 & 0 & 0 & \frac{\Lambda_1}{\delta} \\ 0 & -\mu_T & 0 & 0 & 0 & 0 \\ 0 & 0 & -\mu_1 & 0 & 0 & 0 \\ 0 & 0 & 0 & -\mu_2 & 0 & 0 \\ 0 & 0 & 0 & 0 & -\mu_B & 0 \\ q & q & q & q & q & -\mu_M - \epsilon_S p_S \frac{\Lambda_1}{\delta} \end{bmatrix}.$$

The characteristic polynomial has four trivial eigenvalues given by $-\mu_T$, $-\mu_1$, $-\mu_2$, and $-\mu_B$. The two remaining eigenvalues are those of the 2×2 lower block:

$$J_{22} = \begin{bmatrix} -\mu_S & \frac{\Lambda_1}{\delta} \\ q & -\mu_M - \epsilon_S p_S \frac{\Lambda_1}{\delta} \end{bmatrix}.$$

The trace and determinant of J_{22} are

$$\mathrm{tr}(J_{22}) < 0, \quad \det(J_{22}) = \mu_S \left(\mu_M + \epsilon_S p_S \frac{\Lambda_1}{\delta} \right) - \frac{\Lambda_1 q}{\delta}.$$

Thus, the collapse equilibrium E_0 is locally asymptotically stable if and only if $\det(J_{22}) > 0$, which is equivalent to:

$$\mathcal{R}_0 := \frac{\Lambda_1 q}{\delta \mu_S \mu_M + \epsilon_S p_S \Lambda_1 \mu_S} < 1. \tag{3.1}$$

Remark 1 (Interpretation of the threshold $\mathcal{R}_0$)**.** *The quantity $\mathcal{R}_0$ represents the ratio between the average daily financial inflow into the health system and the economic resistance to screening access. When $\mathcal{R}_0 < 1$, the system lacks sufficient financial throughput to sustain access to the care pathway. When $\mathcal{R}_0 > 1$, available resources allow for effective access to screening and treatment, improving early detection and reducing mortality.*

In what follows, we establish conditions under which the collapse equilibrium E_0 is globally asymptotically stable.

Theorem 2. *The collapse equilibrium $E_0 = (0, 0, 0, 0, 0, 0)$ is globally asymptotically stable in Γ if*

$$\frac{\Lambda_1 q}{\delta \mu_M + \epsilon_S p_S \Lambda_1} \leq \mu, \tag{3.2}$$

where $\mu = \min\{\mu_S, \mu_T, \mu_1, \mu_2, \mu_B\}$.

In particular, if $\mu = \mu_S$*, condition* (3.2) *becomes* $\mathcal{R}_0 \leq 1$ *with* $\mathcal{R}_0$ *defined in* (3.1).

Proof. We construct a Lyapunov function and show that its derivative along the trajectories of system (2.7) is negative definite under condition (3.2). The full proof is given in Appendix A.

Concerning the sustainable equilibrium points, the following holds.

Theorem 3. *System* (2.7) *has*

- *at least one sustainable equilibrium whenever* $\mathcal{R}_0 > 1$*;*
- *one, two, or more sustainable equilibrium points when* $\mathcal{R}_0 < 1$ *(backward bifurcation may occur).*

Proof. Setting $\dot{S}_T = \dot{T}_A = \dot{E}_1 = \dot{E}_2 = \dot{B} = \dot{M} = 0$ gives the algebraic system (B.1). Eliminating S_T, T_A, E_1, E_2, and B expresses each compartment as a function of the single unknown M (B). Substituting these expressions into the $\dot{M} = 0$ equation yields the following degree 8 polynomial:

$$P(M) = M\Big(\sum_{i=0}^{7} X_i M^i\Big) = 0,$$

with $X_7 < 0$ and

$$X_0 = C\,(\mathcal{R}_0 - 1), \qquad C := \mu_1\mu_2\mu_B\mu_S\mu_T^2(2\lambda_1 + \lambda_2)(\delta\mu_S\mu_M + \epsilon_S p_S \Lambda_1 \mu_S) > 0.$$

Hence,

$$\operatorname{sign}(X_0) = \operatorname{sign}(\mathcal{R}_0 - 1).$$

If $\mathcal{R}_0 > 1$, the coefficients $(X_7, \ldots, X_0)$ change sign at least once; by Descartes' rule of signs, $P(M)$ has at least one positive root, so a sustainable equilibrium exists.

If $\mathcal{R}_0 < 1$, $X_0 < 0$ while $X_7 < 0$; depending on intermediate coefficients, $P(M)$ can have 0 or ≥ 2 positive roots, implying possible coexistence of multiple sustainable equilibrium points with the disease-free equilibrium (backward bifurcation).

All algebraic details are given in Appendix B.

3.2. Bifurcation analysis

The phenomenon of backward bifurcation corresponds to a bistable situation in which the system may converge either to the collapse equilibrium or to a sustainable equilibrium depending on the initial conditions. In terms of the economic threshold $\mathcal{R}_0$, this implies that, in a certain parameter region where $\mathcal{R}_0 < 1$, both a sustainable equilibrium and a collapse equilibrium may coexist. From a practical perspective, this means that screening programs may continue to operate even under unfavorable financial conditions. However, such operation remains fragile and highly sensitive to external perturbations, as small variations in initial conditions may lead to a transition toward the collapse equilibrium.

Within the bistable region induced by backward bifurcation, we introduce the following definitions:

Definition 1. *The following definitions are in order:*

- *A conditional resilience zone is the parameter region where a stable sustainable equilibrium and the collapse equilibrium coexist.*

- *A collapse threshold is a critical level of the economic threshold below which the health system converges to the collapse equilibrium, regardless of initial conditions (i.e., initial resource allocation).*
- *An efficient resource allocation within the conditional resilience zone is an initial condition within the basin of attraction of the sustainable equilibrium.*
- *A resource misallocation within the conditional resilience zone is an initial condition within the basin of attraction of the collapse equilibrium.*

Theorem 4. *System* (2.7) *undergoes a backward bifurcation at the critical threshold* $\mathcal{R}_0 = 1$ *if the bifurcation coefficient a defined in* (3.3) *satisfies* $a > 0$. *However, the system exhibits a forward bifurcation at* $\mathcal{R}_0 = 1$ *when* $a < 0$.

Proof. We apply the center manifold theory following the Castillo-Chavez and Song approach [20]. Let q be the bifurcation parameter. Recall from (3.1) that the critical value at $\mathcal{R}_0 = 1$ is

$$q^* = \frac{\delta \mu_S \mu_M}{\Lambda_1} + \epsilon_S p_S \mu_S .$$

We transform system (2.7) into vector notation such that

$$\mathbf{x} = (x_1, x_2, x_3, x_4, x_5, x_6)^T := (S_T, T_A, E_1, E_2, B, M)^T,$$

and,

$$\frac{d\mathbf{x}}{dt} = \mathbf{f}(\mathbf{x}, q),$$

where the explicit form of $\mathbf{f}$ is reproduced in C.

The Jacobian matrix $J(E_0)$ at the disease-free equilibrium $E_0 = 0$ with $q = q^*$ is

$$J(E_0) = \begin{bmatrix} -\mu_S & 0 & 0 & 0 & 0 & \frac{\Lambda_1}{\delta} \\ 0 & -\mu_T & 0 & 0 & 0 & 0 \\ 0 & 0 & -\mu_1 & 0 & 0 & 0 \\ 0 & 0 & 0 & -\mu_2 & 0 & 0 \\ 0 & 0 & 0 & 0 & -\mu_B & 0 \\ q^* & q^* & q^* & q^* & q^* & -\mu_M - \epsilon_S p_S \frac{\Lambda_1}{\delta} \end{bmatrix}.$$

This matrix has four negative eigenvalues and a simple zero eigenvalue coming from the following sub-matrix:

$$J_{22} = \begin{bmatrix} -\mu_S & \frac{\Lambda_1}{\delta} \\ q^* & -\mu_M - \epsilon_S p_S \frac{\Lambda_1}{\delta} \end{bmatrix},$$

with $\det(J_{22}) = 0$ and $\mathrm{tr}(J_{22}) < 0$, confirming that E_0 is nonhyperbolic with a simple zero eigenvalue. The center manifold theory is thus applicable.

Let $\mathbf{w}$ and $\mathbf{v}$ be the right and left eigenvectors associated with the zero eigenvalue, normalized such that $\mathbf{v} \cdot \mathbf{w} = 1$:

$$\mathbf{w} = \left(w_1, 0, 0, 0, 0, \frac{q^*}{\mu_M + \epsilon_S p_S \frac{\Lambda_1}{\delta}} w_1 \right)^T,$$

$$\mathbf{v} = \left(\frac{q^*}{\mu_S}v_6, \frac{q^*}{\mu_T}v_6, \frac{q^*}{\mu_1}v_6, \frac{q^*}{\mu_2}v_6, \frac{q^*}{\mu_B}v_6, v_6\right)^T,$$

with

$$v_6 = \mu_S, \qquad w_1 = \frac{\delta\mu_M + \epsilon_S p_S \Lambda_1}{\epsilon_S p_S \Lambda_1 + \delta(\mu_S + \mu_M)\left(\frac{\delta\mu_M}{\Lambda_1} + \epsilon_S p_S\right)}.$$

Using the formalism in [20], the bifurcation coefficients are

$$b = \sum_{k=1}^{6}\sum_{i=1}^{6} v_k w_i \frac{\partial^2 f_k}{\partial x_i \partial q}(E_0, q^*), \qquad a = \sum_{k=1}^{6}\sum_{i=1}^{6}\sum_{j=1}^{6} v_k w_i w_j \frac{\partial^2 f_k}{\partial x_i \partial x_j}(E_0, q^*).$$

After algebraic calculation, one finds

$$b = v_6 w_1 > 0,$$

and

$$a = \frac{2v_6 w_1^2}{\Lambda_1}\left(\mu_S \epsilon_S p_S + \frac{\alpha_T \delta}{\mu_T} - [q^*(\alpha_T\delta + \mu_S) + \alpha_T \epsilon_T p_T \delta\mu_S)]\right), \tag{3.3}$$

Since $b > 0$, the sign of a determines the bifurcation type: if $a > 0$, the system undergoes a backward bifurcation at $\mathcal{R}_0 = 1$, whereas if $a < 0$, it exhibits only a forward bifurcation.

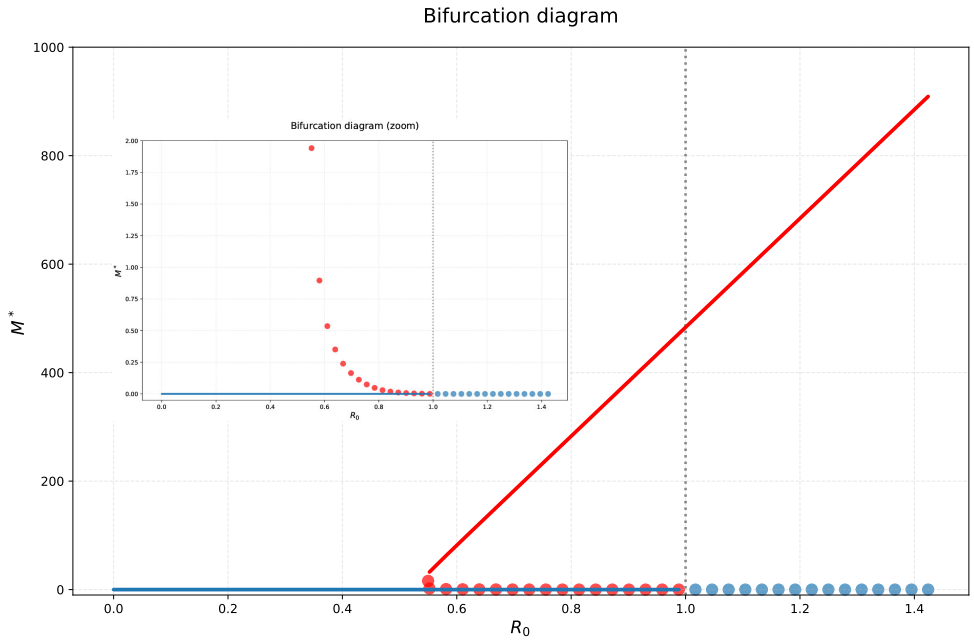

Figure 3. Backward bifurcation diagram. The horizontal axis represents the threshold $\mathcal{R}_0$, and the vertical axis corresponds to the equilibrium value of the state variable M. The red curve represents the sustainable equilibrium, while the blue curve corresponds to the collapse equilibrium. Solid lines indicate stable equilibria, whereas dashed lines represent unstable equilibria. Bistability occurs for $\mathcal{R}_0 \in (0.55, 1)$, where both equilibria coexist. For $\mathcal{R}_0 < 0.55$, the system converges to the collapse equilibrium. For $\mathcal{R}_0 > 1$, the system converges to the stable sustainable equilibrium, indicating the sustainability of the care pathway.

With the parameter values given in Table 2, the condition of existence of a backward bifurcation phenomenon is not observed. However, the analytical results show that a backward bifurcation phenomenon may arise for other parameter sets. From a public health perspective, this result suggests that even when the economic threshold is below one, the system may still maintain screening and treatment activities, at least at a minimal level of functioning, through efficient resource allocation (see Definition 1). Within this conditional resilience zone, the system behaves in two different ways (see Figure 4). The first outcome corresponds to the situation in which screening and treatment activities are maintained despite the fact that the economic threshold is less than one. This behavior is a result of efficient resource allocation across the care pathway. The second corresponds to the collapse of the system. The latter situation may arise in a case of resource misallocation. The presence of a backward bifurcation phenomenon indicates that the government should not be satisfied with the mere normal functioning of the care pathway, as it may simply be operating within a resilience zone in which any misallocation of resources could lead to its collapse. Consequently, the model suggests that policy efforts should focus to drive the economic threshold $\mathcal{R}_0$ above one (by increasing individuals' wage income (q) or by expanding free screening campaigns ($\epsilon_S = 0$)), but also by optimizing resource allocation across different stages of the care pathway in order to ensure convergence toward the sustainable equilibrium.

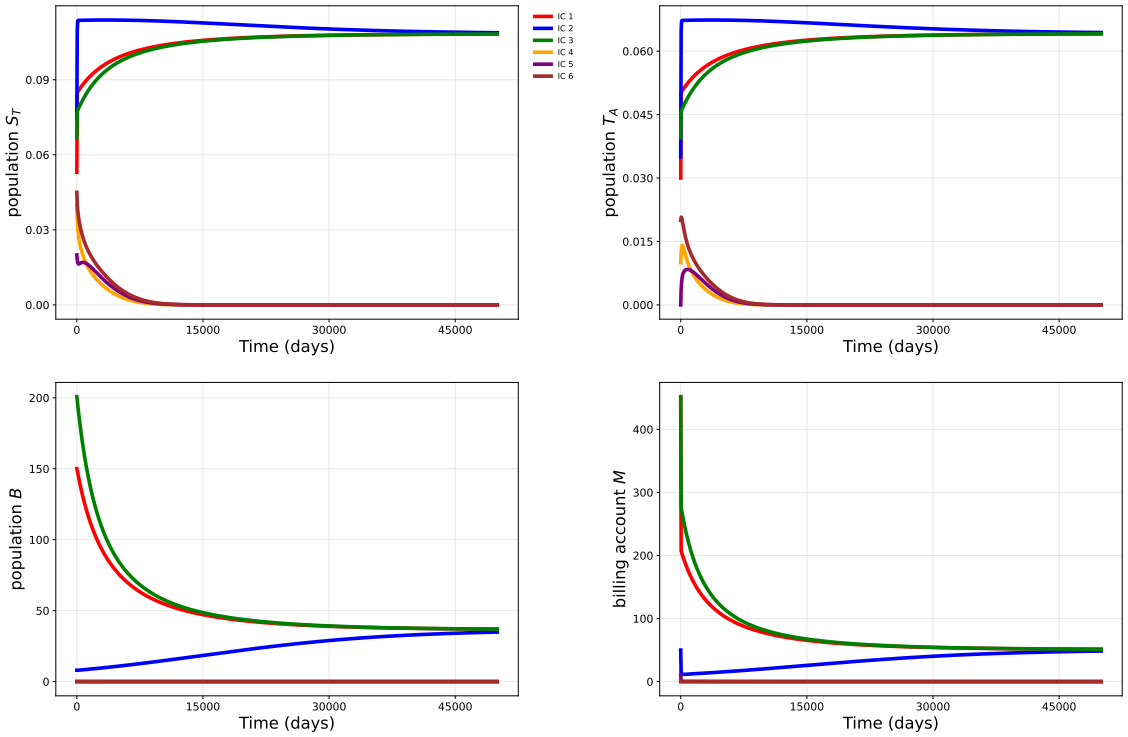

Figure 4. Time evolution of model compartments under six different initial conditions when backward bifurcation occurs. Three solutions (yellow, purple, and brown) converge toward the sustainable equilibrium and three other ones (green, red, and blue) converge toward the collapse equilibrium.

4. Parameter estimation

Parameter values were determined using a combination of literature-based information, simple statistical estimates, and values derived from the economic structure of the healthcare pathway [21, 22]. This approach ensures consistency between the clinical interpretation of the model and the financial mechanisms governing the care pathway.

The total health expenditure per capita in Cameroon is approximately 35,000 XAF per year (around 60 USD), which corresponds to approximately 96 XAF per person per day [23]. Assuming that 10% of this amount is allocated to reproductive and maternal health [24], and that 5% is specifically directed to cervical cancer screening and treatment [25], the resulting allocation per woman is 4.8 XAF per day; then, we have $q = 4.8$ XAF $\cdot day^{-1}$. A screening program may target 70% of women aged 35–45 in Cameroon, and the United Nations World Population Prospects 2024 reports about 1,680,554 women in this age range; hence, 70% corresponds to approximately 1,176,388 women [26]. Most of the transition rates from one stage to another are modeled as the product of a structural parameter (such as γ_1, γ_2, λ_1, λ_2, λ_3, η, β, or α_T) and the financial variable M, representing the available resources. In order to recover consistent values for these parameters, we normalize them by the unit cost of the arrival compartment. This ensures that a transition is only effective if the corresponding financial resources are sufficient to cover the cost of the medical procedure, thus maintaining both dimensional consistency and biological interpretability.

For treatment results, clinical studies in Cameroon report a success rate for thermal ablation of approximately 94% and for LLETZ around 88% [27]. By complementarity, we take 6% failure for thermal ablation and 12% for LLETZ. Consequently, the scaled parameters are $\gamma_1 = 0.94/10{,}000 = 9.4 \times 10^{-5}$, $\gamma_2 = 0.88/10{,}000 = 8.8 \times 10^{-5}$, $\eta = 0.06/5000 = 1.2 \times 10^{-5}$, $\beta = 0.12/30{,}000 = 4 \times 10^{-6}$ (in $\text{XAF}^{-1}\cdot\text{day}^{-1}$). These values are specific to published Cameroonian cohorts, although variability across settings is possible; therefore, uncertainty is considered in sensitivity analysis. Note that γ_1 and γ_2 are normalized by the HPV test cost (p_S), since successful ablation or LLETZ implies a return to the screening compartment S_T.

Using data from the Meskine Mother-Child campaign, the distribution of women with HPV+ and VIA/VILI+ was reported to be approximately 62.5% receiving thermal ablation, 25% undergoing LLETZ, and 12.5% undergoing biopsy [28], we then have $\lambda_1 = 0.625/5000 = 1.25 \times 10^{-4}$, $\lambda_2 = 0.25/20{,}000 = 1.25 \times 10^{-5}$, and $\lambda_3 = 0.125/30{,}000 = 4.16 \times 10^{-6}$ (in $\text{XAF}^{-1}\cdot\text{day}^{-1}$).

For the prevalence of HPV, we use two Cameroonian studies: 19.8% in the Dschang 3T program [29] and 21.43% in a multicenter study (median age 41 years) [30]. Averaging these gives $\alpha_T = 20.6\%$, which divided by the VIA unit cost yields: $\alpha_T = 0.206/5000 = 4.12 \times 10^{-5}$ $\text{XAF}^{-1} \cdot \text{day}^{-1}$.

For mortality rates, the World Bank estimates that the female life expectancy in Cameroon is 65.94 years in 2023 [31]. Using the inverse of life expectancy expressed in days gives a daily mortality rate of $1/(65.94 \times 365) = 4.15 \times 10^{-5}$. We therefore set $\mu_1 = \mu_2 = 4.15 \times 10^{-5}$ day^{-1}.

For the exit rate μ_S in the screened compartment, Biologically, women who test negative are advised to repeat screening after five years. Accordingly, we set $\mu_S = 1/(5 \times 365) = 5.47 \times 10^{-4}$ day^{-1}.

The biopsy compartment may include patients who exit due to death, treatment referral, or loss to follow-up. Assuming an average dwell time of 10 days in this compartment, we estimate: $\mu_B = 0.1$ day^{-1}.

When combining Cameroon Baptist Convention Health Services (CBCHS) with the Dschang 3T site [29, 32], about 33 persons/day were reported in the CBCHS network in 2014 and about 52/day

when both sites were considered. These empirical values suggest that a daily inflow on the order of 50 individuals is operationally feasible in the Cameroonian context, and we therefore set $\Lambda_1 = 50$ persons/day as a realistic baseline consistent with observed program capacities. Finally, the half-saturation constant δ was assumed to be 500 XAF, representing the resource level at which the pathway reaches half of its maximum capacity.

5. Sensitivity analysis

5.1. Sensitivity of the economic threshold

We perform a global sensitivity analysis to identify the most influential parameters affecting the model threshold $\mathcal{R}_0$ defined in Eq (3.1). To achieve this, we combine Latin hypercube Sampling (LHS) with partial rank correlation coefficients (PRCC), a widely used methodology for sensitivity studies in nonlinear and monotonic epidemiological models [33, 34]. LHS is a stratified sampling technique that ensures efficient exploration of the multidimensional parameter space, reducing sampling bias compared to random sampling. A total of 2000 parameter sets were generated within biologically and contextually plausible ranges for the variables appearing in the $\mathcal{R}_0$ expression. For each set, the corresponding value of $\mathcal{R}_0$ was computed. The PRCC method was then applied to measure the strength and direction of the monotonic relationship between each input parameter and the outcome variable $\mathcal{R}_0$, while controlling for the influence of all other parameters [35]. Parameters with high absolute PRCC values and statistically significant p-values (denoted by asterisks in Figure 5) are considered the most influential. A positive PRCC implies that increasing the parameter value increases $\mathcal{R}_0$, whereas a negative PRCC indicates an inverse relationship. This approach has been successfully applied in prior work modeling HIV [36], tuberculosis [37], and other infectious diseases, and proves particularly useful here for guiding policy interventions around cervical cancer screening cost and impact.

According to Figure 5, four parameters have a significant effect: the proportion of the HPV test cost paid by the patient (ϵ_S), the patient's daily contribution to billing account (q), the exit rate in the screened compartment (μ_S), and the cost of the HPV test (p_S). The results show that ϵ_S has a strong negative effect on $\mathcal{R}_0$. This means that when patients have to pay more for the HPV test (because the subsidy is reduced), the system becomes less economically sustainable. This highlights the importance of government support for screening. The patient daily contribution q has a positive effect on $\mathcal{R}_0$, meaning that when patients can save more money each day, it helps them pay for treatment later in the care pathway. The exit rate μ_S has a moderate negative effect, indicating that the low positive screening rate does not help the system, which will remain underfunded because very few people are affected. Finally, the test cost p_S has a negative effect; when the test is too expensive, fewer women get screened, especially in poor regions.

Since the parameter ϵ_S is the most influent parameter, we investigate how its variation can change the values of the basic threshold $\mathcal{R}_0$ when the other parameters are fixed. As illustrated in Figure 6, the threshold $\mathcal{R}_0$ increases monotonically as ϵ_S decreases, confirming the positive impact of government subsidies on screening and treatment pathway. With parameter values given in Table 2, $\mathcal{R}_0 = 1$ is equivalent to $\epsilon_S \approx 0.869$. Literally, the government must cover at least 13.1% of the HPV screening cost to guarantee the long-term economic sustainability of the overall care pathway.

These results show that helping patients pay for screening and encouraging regular savings are both key to making sure cervical cancer prevention services are available to everyone.

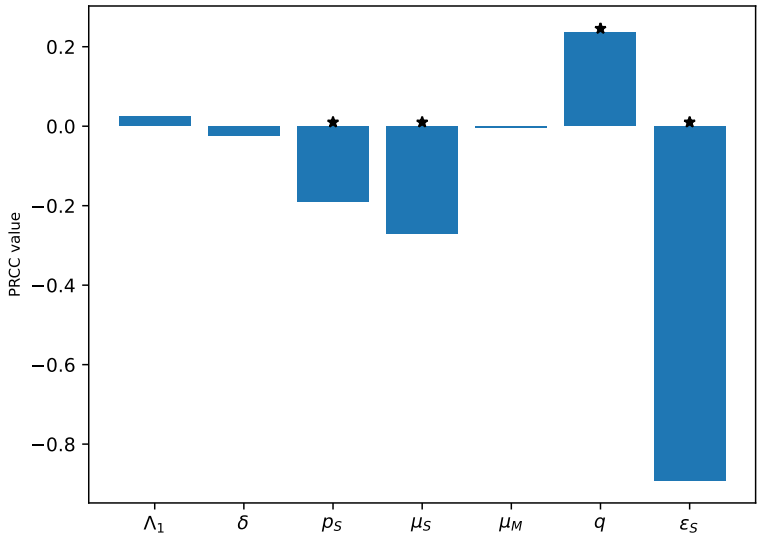

Figure 5. Sensitivity of $\mathcal{R}_0$ to model parameters using PRCC. Asterisks ($*$) indicate parameters with a statistically significant effect at the 5% level. The analysis shows that the patient's share of the HPV test cost (ϵ_S) has the strongest negative impact on $\mathcal{R}_0$, while the daily patient contribution (q) contributes positively. Mortality among screened women (μ_S) and the unit cost of the HPV test (p_S) also have moderate negative effects.

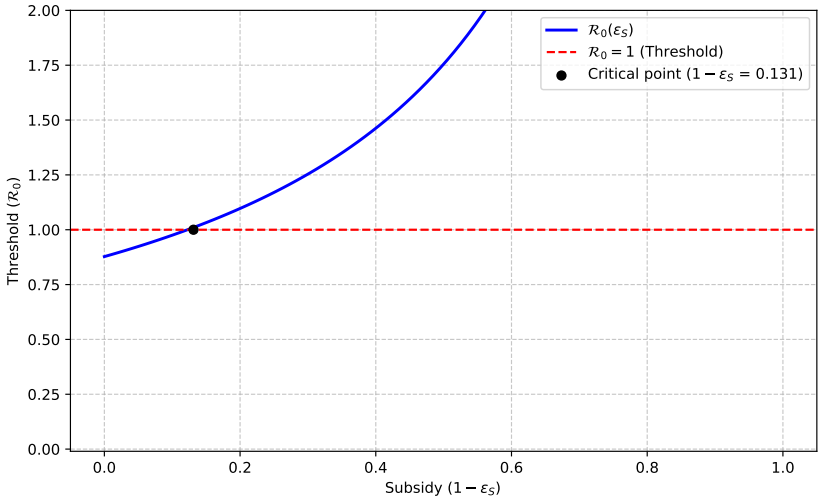

Figure 6. Variation of the threshold $\mathcal{R}_0$ as a function of ϵ_S (patient share of the HPV screening cost).

5.2. Global sensitivity of model dynamics

To assess the relative contribution of each model parameter to the variability of system outputs, we apply the extended Fourier amplitude sensitivity test (eFAST), a global variance-based method particularly suited for nonlinear and nonmonotonic systems [34, 38]. Unlike local sensitivity approaches that perturb one parameter at a time [39], eFAST explores the full parameter space simultaneously and accounts for both direct and interaction effects. This method computes two main indices: the first-order

sensitivity index ($S1$), which measures the direct contribution of each parameter to the output variance, and the total-order sensitivity index (ST), which quantifies the overall contribution of a parameter including its interactions with others. This comprehensive approach enables robust identification of the parameters that most influence the behavior of each state variable in model (2.7). Consequently, these insights guide public health decision-making, notably in prioritizing which parameters require more accurate estimation or policy adjustment. Applications of eFAST in health modeling have proven valuable in low- and middle-income countries where uncertainty quantification is critical for intervention planning [40, 41].

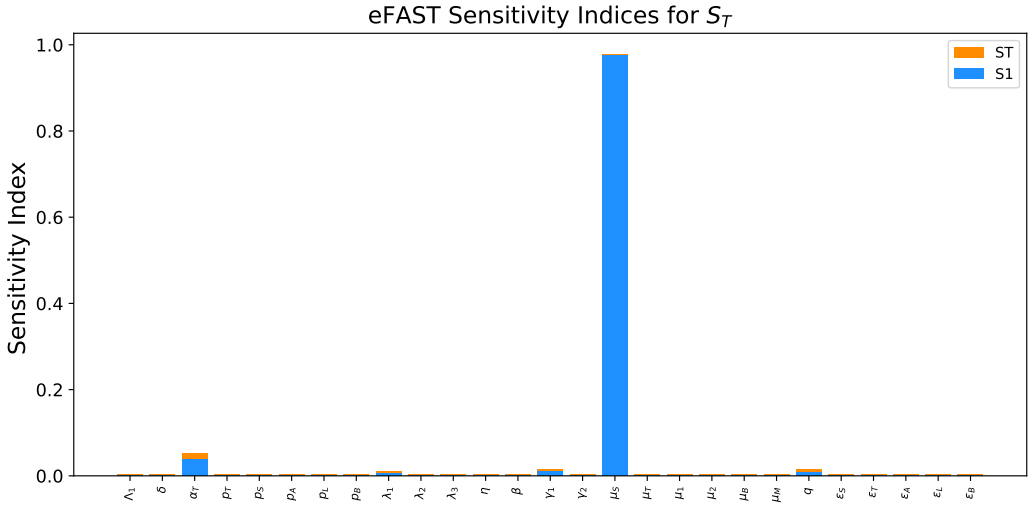

Figure 7. eFAST sensitivity indices for S_T (screened population).

The global sensitivity analysis of (S_T) in Figure 7 shows that the size of the screened population is mainly controlled by the exit rate among the screened compartment (μ_S), the transition rate to eligibility testing (α_T), and also the daily patient contribution (q). These factors indicate that they play an important role in determining how many women remain within the screening compartment. In practice, this means that once women have been screened, their ability to progress further depends on both biological survival and continuous financial contributions, while the gateway to subsequent care is set by the probability of being referred to eligibility testing.

Some other parameters exert a moderate effects, suggesting that the pathway is relatively robust to small variations in treatment costs or success rates once women are already engaged in screening. On the other hand, structural constants such as the maximum inflow rate (Λ_1) or the half-saturation threshold (δ) have negligible impact, which implies that financial and biological constraints dominate over theoretical capacity limits in shaping the screening pool.

Since the downstream cost of treatment depends directly on the fraction of screened women who test positive and transition to eligibility testing, any increase in α_T or reduction in financial barriers (q) could substantially raise the number of women progressing to T_A. As a result, while these mechanisms improve access to care, they are also likely to absorb a large share of the total budget in subsequent stages. In other words, the sensitivity profile of S_T anticipates that the bulk of program expenditures will be driven not by the absolute number of women entering screening, but by the proportion that can successfully advance toward treatment or exit the pathway.

According to Figure 8, the billing account M is strongly shaped by the following parameters:

the transition rate to eligibility testing (α_T), the unit cost of HPV screening (p_S), the daily patient contribution (q), and the level of subsidy for HPV testing (ϵ_S). Each of these factors directly determines the inflow and outflow of money: α_T sets how many screened women require further resources for a VIA test, q reflects the continuous contributions that replenish the account, while p_S and ϵ_S govern how much funding is consumed at the initial stage of testing. All other parameters display negligible sensitivity, suggesting that once patients move beyond the eligibility test, the billing account is relatively insensitive to variation in downstream treatment costs.

These imply that the long-term sustainability of the billing account is primarily dictated by the dynamics of early detection. Higher values of α_T increase the financial demand by sending more women to eligibility test for ablative treatment and subsequent care, while stronger patient contributions or subsidies can stabilize the balance by reducing costs at the screening stage. This sensitivity profile anticipates that overall program costs will be absorbed mainly by the combination of how many women progress beyond screening and how much financial relief is provided at the very first test.

The complete sensitivity analysis results for T_A (women receiving VIA), E_1 (women receiving ablative treatment), E_2 (women receiving LLETZ), and B (women undergoing biopsy) are presented in Appendix D, together with their corresponding visual representations.

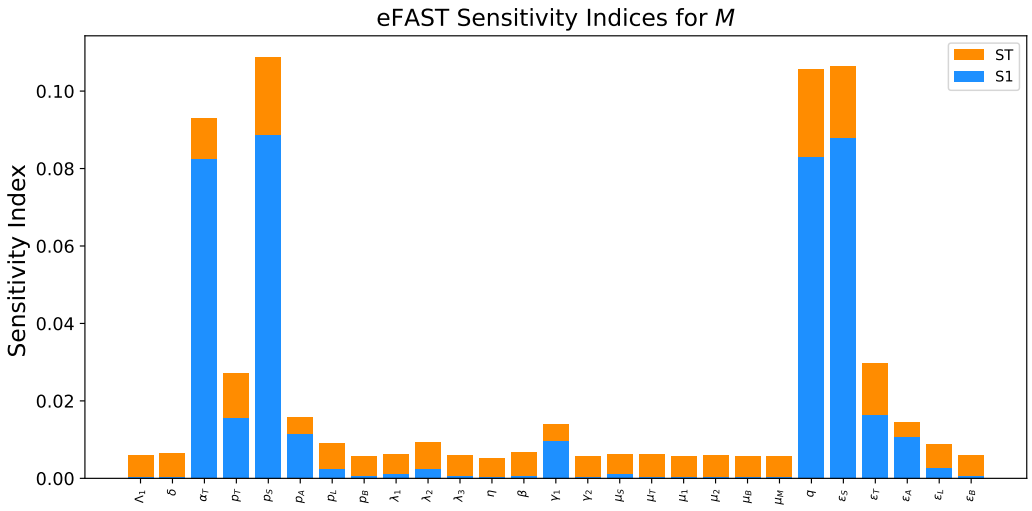

Figure 8. eFAST sensitivity indices for billing account.

6. Estimation and optimization of the total treatment cost

In this section, we estimate the cost of screening and treatment for precancerous cervical lesions using a dynamic simulation-based approach. Instead of focusing only on equilibrium values, we compute the treatment cost by summing all expenditures incurred over time, as dictated by the model's resource flows.

Specifically, at each time t, the instantaneous financial outflows are defined by the expenditure terms in the equation for $\dot{M}(t)$ (see Eq (2.7)). These include costs associated with screening, treatment interventions, biopsies, and system maintenance. We then set the following metrics corresponding to stage-specific outflow costs:

- HPV screening:

$$C_{S_T}(t) = \epsilon_S p_S \left(\frac{\Lambda_1 M(t)}{\delta + M(t)} + \gamma_1 M(t) E_1(t) + \gamma_2 M(t) E_2(t) \right).$$

- Eligibility test for ablative treatment:

$$C_{T_A}(t) = \epsilon_T p_T \left(\alpha_T M(t) S_T(t) + \eta M(t) E_1(t) \right).$$

- Ablative treatment:

$$C_{E_1}(t) = \epsilon_A p_A \lambda_1 M(t) T_A(t).$$

- LLETZ treatment:

$$C_{E_2}(t) = \epsilon_L p_L \lambda_2 M(t) T_A(t).$$

- Biopsies:

$$C_B(t) = \epsilon_B p_B \left(\lambda_3 M(t) T_A(t) + \beta M(t) E_2(t) \right).$$

- Natural depletion:

$$C_{\text{op}}(t) = \mu_M M(t).$$

The total instantaneous cost is then

$$C(t) = C_{S_T}(t) + C_{T_A}(t) + C_{E_1}(t) + C_{E_2}(t) + C_B(t) + C_{\text{op}}(t).$$

Finally, the total cost over a period $[0, T]$, says $C_{\text{total}}(T)$, is obtained via the following integration:

$$C_{\text{total}}(T) = \int_0^T C(t)\, dt. \tag{6.1}$$

This dynamic approach provides a clearer way to compare different policy options, such as subsidy levels or screening strategies, over a defined period of time. In practice, we visualize the evolution of $C_{\text{total}}(T)$ over time and provide a decomposition by stage to identify which interventions dominate the cost profile. To gain deeper insight into how resources are allocated across the different stages of care, we further estimate the number of women passing through each stage of the treatment pathway over the simulation period, as well as the average cost per woman for each component.

For each intervention (screening, eligibility testing, treatment, etc.), we compute the number of women who receive that intervention by integrating the corresponding flow of entry into the associated compartment. For instance, the total number of women screened over the horizon $[0, T]$ is given by

$$N_{\text{screened}} = S_T(0) + \int_0^T \left(\frac{\Lambda_1 M(t)}{\delta + M(t)} + \gamma_1 M(t) E_1(t) + \gamma_2 M(t) E_2(t) \right) dt.$$

Similarly, we compute N_{tested}, N_{ablated}, N_{LLETZ}, and N_{biopsied} by integrating the inflow terms associated with each respective stage. The numerical results of this analysis are presented and discussed in the following.

6.1. Forecast in 10 years

Using the dynamic integration-based approach described above, we estimated the cost of screening and treatment of precancerous cervical lesions over a 10-year period, assuming no government subsidies ($\epsilon_X = 1$ for all stages). This time horizon was chosen to align with the World Health Organization's global strategy to eliminate cervical cancer, which established the 90–70–90 targets for the year 2030, launched in 2020. The simulation results show that the total expenditure over $T = 3650$ days amounts to

$$C_{\text{total}}(10 \text{ years}) \approx 23.07 \times 10^9 \text{ XAF}.$$

A detailed breakdown of the simulated costs indicates that HPV screening constitutes the dominant share of total expenditures (approximately 15.54 billion XAF corresponding to 67.4% of the overall cost), followed by the eligibility test (3.33 billion XAF corresponding to 14.5% of the overall cost), ablative treatment (2.59 billion XAF corresponding to 11.2% of the overall cost), LLETZ treatment (1.04 billion XAF, corresponding to 4.5% of the overall cost), and biopsies (564 million XAF, corresponding to 2.4% of the overall cost). Operational losses due to natural depletion are negligible.

In terms of patient flow, the model predicts that over a 10-year period, approximately 1,554,221 HPV screening tests would need to be performed, along with 667,050 eligibility tests for ablative treatment, 517,779 ablation procedures, 51,778 LLETZ interventions, and 18,813 biopsies.

These results highlight that HPV screening and eligibility testing together absorb nearly 80% of total expenditures. Therefore, introducing targeted subsidies at these stages could substantially reduce the global financial burden while maintaining program coverage and sustainability. This decomposition also provides a quantitative basis for the optimization framework presented in the next section, where subsidy levels are calibrated to minimize C_{total} under the constraint $\mathcal{R}_0 > 1$.

6.2. Optimal allocation of subsidies that minimize treatment costs

In this section, we focus on determining the optimal allocation of government subsidies across the different stages of the precancerous cervical lesions care pathway in order to minimize the treatment cost while ensuring the long-term sustainability of the system.

Let us consider θ_S, θ_T, θ_A, θ_L, and θ_B, corresponding to the HPV test subsidy, eligibility test subsidy, the ablative treatment subsidy, the LLETZ treatment subsidy, and biopsy subsidy respectively. According to our modeling, these variables have the form $\theta_X = 1 - \epsilon_X$, where ϵ_X is the proportion of the cost paid by the patient with $X \in \{S, T, A, L, B\}$, and it varies within the range $[0, 1]$.

Since the sustainability condition of the care pathway imposes a minimal subsidy for the HPV test, θ_S is fixed at that level of 0.131. The remaining subsidies are allocated following the optimization problem:

$$\begin{cases} \min\limits_{\theta_T,\theta_A,\theta_L,\theta_B} \quad C_{\text{total}}(T) \\ \text{subject to:} \quad \dfrac{N_{\text{ablated}}(T) + N_{\text{LLETZ}}(T) + N_{\text{biopsied}}(T)}{N_{\text{tested}}(T)} = 0.90, \\ \qquad\qquad 0 \le \theta_X \le 1, \quad X \in \{T, A, L, B\}. \end{cases} \tag{6.2}$$

The constraint of the optimization problem ensures that 90% of the women who have been tested for eligibility (N_{tested}) are taken care of, either through ablation, LLETZ, or biopsy. This constraint

is based on the 90-70-90 targets set by the World Health Organization (WHO) for cervical cancer prevention [42], specifically adapted to the context of Cameroon. According to the WHO's Global Strategy for the Elimination of Cervical Cancer as a Public Health Problem, the objective is to ensure that 90% of girls aged 9–14 years are fully vaccinated against HPV, to ensure that 70% of women aged 35–45 years are screened with a high-performance HPV test, and to ensure that 90% of women identified with precancerous lesions or cervical cancer receive appropriate treatment, starting from the T_A class in our model.

In the context of this study, the 90% coverage constraint focuses on ensuring that a sufficient proportion of women who test positive for HPV are indeed taken care of in the next stages. This aligns with the WHO's strategic objective to achieve a high level of access to treatment and prevent the progression of cervical lesions to cancer.

6.3. Results of the optimization problem

The optimization aimed to minimize the treatment cost while ensuring that 90% of the women who tested positive for HPV are adequately treated. Problem (6.2) has been solved numerically with parameter values given in Table 2. We found the following optimal subsidies: $\theta_T = 27.75\%$, $\theta_A = 25.82\%$, $\theta_L = 35.14\%$, and $\theta_B = 0.00\%$. This allocation ensures that the required subsidy levels for each stage of care are determined, guaranteeing that 90% of women who test positive for HPV receive the necessary treatment.

To ensure achievement of the 90% coverage target, the total treatment cost was minimized while maintaining the optimal subsidy levels. By calculating the proportion of the total cost that the government must finance, we first determined the government's contribution to each stage of the treatment process. Specifically, the government covers 13.1% of the HPV screening cost, 27.75% of the eligibility test cost, 25.82% of the ablation cost, 35.14% of the LLETZ cost, and 0% of the biopsy cost. These contributions amounted to a total of 4,994,234,864.93 XAF, which represents approximately 21.65% of the total treatment cost expected without subsidies. This highlights the crucial role of government funding in making cervical cancer prevention and treatment both accessible and sustainable.

7. Conclusions

This study developed an economic-epidemiological model describing the care pathway for precancerous cervical lesions in low- and middle-income countries. The model explicitly combines the clinical progression of patients with their financial capacity, through a dynamic patient billing account that regulates access to each stage of the care pathway. This formulation makes it possible to represent, in a realistic way, the interdependence between health financing and the continuity of preventive programs.

From a theoretical point of view, we established the main mathematical properties of the model, including the positivity and boundedness of all variables, and derived the basic economic threshold $\mathcal{R}_0$ that determines the long-term sustainability of the care system. The analysis revealed the existence of a backward bifurcation, showing that even when $\mathcal{R}_0 < 1$, the system can sustain or collapse depending on initial conditions. The global stability of the collapse equilibrium was also demonstrated under specific conditions.

Sensitivity analyses using PRCC and eFAST highlighted that the parameters most influencing system performance are those directly linked to patient costs, particularly the price of the HPV screening

test, the level of public subsidy, and the patient contribution rate to the billing account. Numerical simulations confirmed that a sufficient level of financial support for screening can shift the system from collapse to a sustainable state, underscoring the central role of economic accessibility.

A numerical optimization problem was formulated to determine the optimal allocation of government subsidies across the various stages of the care pathway, with the primary goal of minimizing treatment costs while ensuring that 90% of women tested positive for HPV are appropriately treated. The results indicate that the optimal subsidy levels prioritize critical stages, such as the LLETZ treatment and eligibility testing, while allocating minimal subsidies to the biopsy stage. The optimization reveals that in order to achieve 90% coverage for those in need, the government must cover approximately 21.65% of the total treatment cost, distributed across the stages according to the optimal subsidy rates. This highlights the crucial role of targeted subsidies in ensuring both accessibility and financial sustainability of cervical cancer prevention and treatment.

Finally, this modeling framework provides a comprehensive tool to analyze and optimize preventive care strategies under financial constraints. By linking economic factors to epidemiological outcomes, it enables policymakers to quantify the effects of subsidies, assess the sustainability of current programs, and explore alternative funding scenarios. The results highlight that financial barriers remain a key determinant of access to cervical cancer screening in low- and middle-income countries, and that strategic public investment in early detection is essential to ensure long-term program viability. In this study, government subsidies are modeled in a very simple way. The financial inflow is modeled as a function of the number of patients (qN), reflecting decentralized financing mechanisms largely based on out-of-pocket payments. Even though this assumption is consistent with the Cameroonian context, it does not capture alternative financing structures based on fixed or externally allocated budgets. An extension of the model would therefore consist of introducing a constant financial inflow, representing a fixed governmental or institutional budget. Furthermore, financial accessibility is assumed to be the primary barrier to treatment access. In practice, healthcare systems in many low- and middle-income countries may also face capacity constraints related to medical infrastructure, equipment availability, or trained personnel. Incorporating such constraints into the model represents an important direction for further work.

Use of AI tools declaration

The authors declare they have not used Artificial Intelligence (AI) tools in the creation of this article.

Author contributions

Marius Tadjuidje Fodjo: Conceptualization, Methodology, Formal analysis, Visualization, Writing-original draft. Aurelien Kambeu Youmbi: Methodology, Formal analysis, Visualization, Writing – review & editing, Supervision. Maison Mayeh: Investigation, Resources, Writing – review & editing. Solange Whegang: Investigation, Writing – review & editing. Bruno Kenfack: Investigation, Resources, Writing – review & editing. Berge Tsanou: Conceptualization, Methodology, Supervision, Funding acquisition, Writing – review & editing.

Data availability statement

The data used for this research were either extracted from biological and economic literature, or estimated based on the knowledge on the research questions being investigated.

Acknowledgments

This research was conducted at the University of Dschang, as part of the Central and Eastern Africa Female Health Oriented Modeling Epidemics Consortium (CAFHOMEC) Project. This work was supported by the Bill & Melinda Gates Foundation, United States (CAFHOMEC project, Grant No. INV-022584).

Conflict of interest

The authors declare there are no conflicts of interest.

References

1. *World Health Organization*, *Cervical Cancer*, 2024. Available from: https://www.who.int/news-room/fact-sheets/detail/cervical-cancer.
2. R. Hull, M. Mbele, T. Makhafola, C. Hicks, S. M. Wang, R. M. Reis, et al., Cervical cancer in low and middle-income countries, *Oncol. Lett.*, **20** (2020), 2058–2074. https://doi.org/10.3892/ol.2020.11754
3. *World Health Organization*, *Cervical Cancer*, 2023. Available from: https://www.who.int/news-room/fact-sheets/detail/cervical-cancer.
4. C. Ngalla, F. Manjuh, J. F. L. Elit, Clinical outcomes of women who attend the Cameroon Baptist Convention Health Services (CBCHS) with cervical cancer, *Biomed. J. Sci. Tech. Res.*, **49** (2023), 40328–40337. https://doi.org/10.26717/BJSTR.2023.49.007753
5. A. M. M. Mayeh, B. S. E. Mapoko, R. R. M. Mapenya, A. J. F. Sango, E. D. B. Mbassi, E. A. Okobalemba, et al., Coût réel de la prise en charge des cancers du col de l'utérus en radiothérapie au Cameroun, *Health Sci. Dis.*, **24** (2023), 109–113. https://doi.org/10.5281/hsd.v24i1.4143
6. G. Litjens, T. Kooi, B. E. Bejnordi, A. A. A. Setio, F. Ciompi, M. Ghafoorian, et al., A survey on deep learning in medical image analysis, *Med. Image Anal.*, **42** (2017), 60–88. https://doi.org/10.1016/j.media.2017.07.005
7. B. S. E. Mapoko, A. M. M. Mayeh, R. R. M. Mapenya, E. D. B. Mbassi, E. A. Okobalemba, A. J. F. Sango, et al., Aspects épidémiologiques et cliniques des cancers du col de l'utérus au Cameroun: Expérience de l'Hôpital Général de Douala, *Pan Afr. Med. J.*, **42** (2022), 109. https://doi.org/10.11604/pamj.2022.42.109.30704
8. P. M. Tebeu, J. S. S. Antaon, M. Adjeba, F. Pikop, J. T. Fouogue, P. Ndom, Connaissances, attitudes et pratiques des professionnels de santé sur le cancer du col de l'utérus au Cameroun, *Santé Publique*, **32** (2021), 489–496. https://doi.org/10.3917/spub.205.0489

9. T. Sefuthi, L. Nkonki, A systematic review of economic evaluations of cervical cancer screening methods, *Syst. Rev.*, **11** (2022), 162. https://doi.org/10.1186/s13643-022-02017-z
10. N. G. Campos, M. Sharma, A. Clark, K. Lee, F. Geng, C. Regan, et al., The health and economic impact of scaling cervical cancer prevention in 50 low- and lower-middle-income countries, *Int. J. Cancer*, **144** (2019), 2961–2970. https://doi.org/10.1002/ijc.32097
11. J. Sherris, S. Wittet, A. Kleine, J. Sellors, S. Luciani, Evidence-based, alternative cervical cancer screening approaches in low-resource settings, *Vaccine*, **39** (2021), 7302–7310. https://doi.org/10.1016/j.vaccine.2021.10.025
12. R. K. Rai, A. K. Misra, Y. Takeuchi, Modeling the impact of sanitation and awareness on the spread of infectious diseases, *Math. Biosci. Eng.*, **16** (2019), 667–700. https://doi.org/10.3934/mbe.2019032
13. *World Health Organization*, WHO algorithm for primary HPV DNA test screening for general population of women, in *WHO Guideline for Screening and Treatment of Cervical Pre-cancer Lesions for Cervical Cancer Prevention*, 2nd edition, 2021. Available from: https://www.ncbi.nlm.nih.gov/books/NBK572308/.
14. *World Health Organization*, *WHO Guideline for Screening and Treatment of Cervical Pre-cancer Lesions for Cervical Cancer Prevention*, 2nd edition, Geneva, 2021. Available from: https://www.who.int/publications/i/item/9789240030824.
15. *Gouvernement de la République du Cameroun*, *Décret n° 2024/0168/PM du 23 Février 2024 Fixant le Salaire Minimum Interprofessionnel Garanti (SMIG) au Cameroun*, 2024. Available from: https://www.spm.gov.cm/site/?q=fr/content-finder/decret_ndeg_2024_0168.pdf.
16. C. S. Holling, The components of predation as revealed by a study of small-mammal predation of the European pine sawfly, *Can. Entomol.*, **91** (1959), 293–320. https://doi.org/10.4039/Ent91293-5
17. A. Ntembe, R. Tawah, E. Faux, Redistributive effects of health care out-of-pocket payments in Cameroon, *Int. J. Equity Health*, **20** (2021), 227. https://doi.org/10.1186/s12939-021-01562-8
18. L. Elit, F. Manjuh, L. Kila, B. Suika, M. Sinou, E. Bozy, et al., Mother–child approach to cervical cancer prevention in a low resource setting: The Cameroon Baptist Convention Health Services story, *Curr. Oncol.*, **31** (2024), 3227–3238. https://doi.org/10.3390/curroncol31060244
19. D. G. Luenberger, *Introduction to Dynamic Systems: Theory, Models, and Applications*, John Wiley & Sons, New York, 1979.
20. C. Castillo-Chavez, B. Song, Dynamical models of tuberculosis and their applications, *Math. Biosci. Eng.*, **1** (2004), 361–404. https://doi.org/10.3934/mbe.2004.1.361
21. F. Saldana, J. A. Camacho-Gutierrez, G. Villavicencio-Pulido, J. X. Velasco-Hernandez, Modeling the transmission dynamics and vaccination strategies for human papillomavirus infection: An optimal control approach, *Appl. Math. Model.*, **112** (2022), 767–785. https://doi.org/10.1016/j.apm.2022.08.017
22. A. K. Youmbi, S. Touzeau, F. Grognard, B. Tsanou, Self-financing model for cabbage crops with pest management, *Math. Biosci.*, **378** (2024), 109332. https://doi.org/10.1016/j.mbs.2024.109332
23. *World Health Organization*, *Global Health Expenditure Database*, 2024. Available from: https://apps.who.int/nha/database.

24. *Ministry of Public Health and National Institute of Statistics*, *Demographic and Health Survey 2018: Cameroon, Cameroon Ministry of Public Health*, 2019. Available from: https://dhsprogram.com/publications/publication-FR360-DHS-Final-Reports.cfm.

25. *World Health Organization*, *Comprehensive Cervical Cancer Control: A Guide to Essential Practice*, 2nd edition, World Health Organization, 2014. Available from: https://www.who.int/publications/i/item/9789241548953.

26. *United Nations, Department of Economic and Social Affairs, Population Division*, *Cameroon Demographics 2024 - Population by Age and Sex (UN WPP 2024)*, 2024. Available from: https://statisticstimes.com/demographics/country/cameroon-demographics.php.

27. J. F. Nkfusai, S. M. Manga, K. Nulah, C. Ngalla, F. Manjuh, N. C. Nkfusai, et al., Cervical precancer treatment outcomes in Cameroon, *Int. J. Matern. Child Health AIDS*, **13** (2024), e020. https://doi.org/10.25259/IJMA_8_2024

28. L. Elit, F. Manjuh, L. Kila, B. Suika, M. Sinou, E. Bozy, et al., Mother–child approach to cervical cancer prevention in a low resource setting: The Cameroon Baptist Convention Health Services story, *Curr. Oncol.*, **31** (2024), 3227–3238. https://doi.org/10.3390/curroncol31060244

29. J. Levy, M. de Preux, B. Kenfack, J. Sormani, R. Catarino, E. F. Tincho, et al., Implementing the 3T-approach for cervical cancer screening in Cameroon: Preliminary results on program performance, *Cancer Med.*, **9** (2020), 7293–7300. https://doi.org/10.1002/cam4.3355

30. M. C. T. Tchouaket, J. Fokam, S. M. Sosso, E. N. J. Semengue, B. Yagai, R. K. Simo, et al., High genotypic diversity of human papillomavirus among women in Cameroon: Implications for vaccine effectiveness, *IJID Reg.*, **5** (2022), 130–136. https://doi.org/10.1016/j.ijregi.2022.09.014

31. *CEIC, Cameroon CM: Life Expectancy at Birth: Female*, 2023. Available from: https://www.ceicdata.com/en/cameroon/social-health-statistics/cm-life-expectancy-at-birth-female.

32. G. DeGregorio, S. Manga, E. Kiyang, F. Manjuh, L. Bradford, P. Cholli, et al., Implementing a fee-for-service cervical cancer screening and treatment program in Cameroon: Challenges and opportunities, *Oncologist*, **22** (2017), 850–859. https://doi.org/10.1634/theoncologist.2016-0383

33. S. M. Blower, H. Dowlatabadi, Sensitivity and uncertainty analysis of complex models of disease transmission: An HIV model, as an example, *Int. Stat. Rev.*, **62** (1994), 229–243. https://doi.org/10.2307/1403510

34. S. Marino, I. B. Hogue, C. J. Ray, D. E. Kirschner, A methodology for performing global uncertainty and sensitivity analysis in systems biology, *J. Theor. Biol.*, **254** (2008), 178–196. https://doi.org/10.1016/j.jtbi.2008.04.011

35. J. Wu, R. Dhingra, M. Gambhir, J. V. Remais, Sensitivity analysis of infectious disease models: Methods, advances and their application, *J. R. Soc. Interface*, **10** (2013), 20121018. https://doi.org/10.1098/rsif.2012.1018

36. Z. Chazuka, C. E. Madubueze, D. Mathebula, Modeling and analysis of an HIV model with control strategies and cost-effectiveness, *Results Control Optim.*, **14** (2024), 100355. https://doi.org/10.1016/j.rico.2023.100355

37. Y. Wu, T. Yang, D. Xu, X. Zhang, L. Guo, Y. Wang, et al., The prevention and control of tuberculosis: An analysis based on sensitivity and uncertainty, *BMC Public Health*, **20** (2020), 926. https://doi.org/10.1186/s12889-020-09260-w

38. A. Saltelli, K. Chan, E. M. Scott, *Sensitivity Analysis*, Wiley, 2000.

39. N. Chitnis, J. M. Hyman, J. M. Cushing, Determining important parameters in the spread of malaria through the sensitivity analysis of a mathematical model, *Bull. Math. Biol.*, **70** (2008), 1272–1296. https://doi.org/10.1007/s11538-008-9299-0

40. B. Iooss, P. Lemaître, A review on global sensitivity analysis methods, in *Uncertainty Management in Simulation-Optimization of Complex Systems: Algorithms and Applications* (eds. G. Dellino and C. Meloni), Springer, Boston, MA, (2015), 101–122. https://doi.org/10.1007/978-1-4899-7547-8_5

41. A. Olivares, E. Staffetti, Uncertainty quantification of a mathematical model of COVID-19 transmission dynamics with mass vaccination strategy, *Chaos, Solitons Fractals*, **146** (2021), 110895. https://doi.org/10.1016/j.chaos.2021.110895

42. *World Health Organization*, *Global Strategy to Accelerate the Elimination of Cervical Cancer as A Public Health Problem*, World Health Organization, Geneva, 2020. Available from: https://www.who.int/publications/i/item/9789240014107.

Appendix

A. Proof of global stability via Lyapunov function

We consider the Lyapunov candidate:

$$V(S_T, T_A, E_1, E_2, B, M) = q(S_T + T_A + E_1 + E_2 + B) + \alpha_6 M,$$

with $\alpha_6 > 0$ to be determined.

Computing $\dot{V}$ along the trajectories of system (2.7) gives

$$\begin{aligned}\dot{V} = q&\left[\frac{\Lambda_1 M}{\delta + M} - \mu_S S_T - \mu_T T_A - \mu_1 E_1 - \mu_2 E_2 - \mu_B B\right] \\ &+ \alpha_6\left[qN - \mu_M M - \epsilon_S p_S\left(\frac{\Lambda_1 M}{\delta + M} + \gamma_1 M E_1 + \gamma_2 M E_2\right)\right. \\ &\left. - \epsilon_T p_T(\alpha_T M S_T + \eta M E_1) - \epsilon_A p_A \lambda_1 M T_A - \epsilon_L p_L \lambda_2 M T_A - \epsilon_B p_B(\lambda_3 M T_A + \beta M E_2)\right].\end{aligned}$$

To ensure $\dot{V} < 0$, we impose

$$\frac{\Lambda_1 q}{\delta\mu_M + \epsilon_S p_S \Lambda_1} \leq \alpha_6 \leq \mu.$$

This leads to

$$\begin{aligned}\dot{V} < \frac{\Lambda_1 q M}{\delta + M} + \alpha_6&\left[-\mu_M M - \epsilon_S p_S\left(\frac{\Lambda_1 M}{\delta + M} + \gamma_1 M E_1 + \gamma_2 M E_2\right)\right. \\ &\left. - \epsilon_T p_T(\alpha_T M S_T + \eta M E_1) - \epsilon_A p_A \lambda_1 M T_A - \epsilon_L p_L \lambda_2 M T_A - \epsilon_B p_B(\lambda_3 M T_A + \beta M E_2)\right],\end{aligned}$$

from which we deduce

$$\begin{aligned}\dot{V} < &-\frac{\mu_M M^2}{\delta + M} - \epsilon_S p_S \left(\gamma_1 M E_1 + \gamma_2 M E_2\right) - \epsilon_L p_L \lambda_2 T_A M \\ &- \epsilon_T p_T \left(\alpha_T M S_T + \eta M E_1\right) - \epsilon_A p_A \lambda_1 M T_A - \epsilon_B p_B (\lambda_3 M T_A + \beta M E_2) \\ &< 0.\end{aligned}$$

Thus, V is a strict Lyapunov function on Γ, and global asymptotic stability follows.

B. Detailed derivation of the sustainable equilibrium

We provide here the complete algebraic steps leading to the expression of the sustainable equilibrium, under the assumption that $M > 0$ and all other compartments are strictly positive.

At equilibrium, we set the right-hand sides of the model (2.7) to zero. The equations for the five epidemiological variables become

$$\begin{cases} 0 = \frac{\Lambda_1 M}{\delta + M} + \gamma_1 M E_1 + \gamma_2 M E_2 - \alpha_T M S_T - \mu_S S_T, \\ 0 = \alpha_T M S_T + \eta M E_1 - (\lambda_1 + \lambda_2 + \lambda_3) M T_A - \mu_T T_A, \\ 0 = \lambda_1 M T_A - \gamma_1 M E_1 - \eta M E_1 - \mu_1 E_1, \\ 0 = \lambda_2 M T_A - \gamma_2 M E_2 - \beta M E_2 - \mu_2 E_2, \\ 0 = \lambda_3 M T_A + \beta M E_2 - \mu_B B. \end{cases} \tag{B.1}$$

From the third and fourth equations,

$$E_1 = \frac{\lambda_1 M T_A}{\gamma_1 M + \eta M + \mu_1}, \qquad E_2 = \frac{\lambda_2 M T_A}{\gamma_2 M + \beta M + \mu_2}.$$

From the fifth,

$$B = \frac{\lambda_3 M T_A + \beta M E_2}{\mu_B}.$$

Substitute E_1 into the second equation, isolate T_A:

$$T_A = \frac{1}{\mu_T + \lambda M} \left[\alpha_T M S_T + \eta M E_1\right], \quad \text{where } \lambda = \lambda_1 + \lambda_2 + \lambda_3.$$

From the first equation,

$$S_T = \frac{1}{\mu_S + \alpha_T M} \left[\frac{\Lambda_1 M}{\delta + M} + \gamma_1 M E_1 + \gamma_2 M E_2\right].$$

We now aim to eliminate all variables in favor of M only.

First, rewrite E_1 in terms of E_2:

$$E_1 = \frac{\lambda_1 (\gamma_2 M + \beta M + \mu_2)}{\lambda_2 (\gamma_1 M + \eta M + \mu_1)} E_2.$$

Let

$$g(M) = \frac{\lambda_1(\gamma_2 M + \beta M + \mu_2)}{\lambda_2(\gamma_1 M + \eta M + \mu_1)}.$$

Then,

$$E_1 = g(M)E_2.$$

Now plug S_T, E_1, and E_2 into the expression for T_A:

$$T_A = \frac{1}{\mu_T + \lambda M}\left[\alpha_T M S_T + \eta M g(M) E_2\right].$$

Also:

$$S_T = \frac{1}{\mu_S + \alpha_T M}\left[\frac{\Lambda_1 M}{\delta + M} + \gamma_1 M g(M) E_2 + \gamma_2 M E_2\right].$$

By substituting all expressions into the conservation equation identity (sum of the five $\dot{X} = 0$), and collecting terms, we arrive at the following equation:

$$\frac{\Lambda_1 M}{\delta + M} = a(M)S_T + b(M)E_1 + c(M)E_2,$$

with

$$a(M) = \mu_S + \frac{(\mu_T + \lambda_3 M)\alpha_T M}{\mu_T + \lambda M}, \quad b(M) = \mu_1 + \frac{(\mu_T + \lambda_3 M)\eta M}{\mu_T + \lambda M}, \quad c(M) = \mu_2 + \beta M.$$

Replacing S_T, E_1 by their expressions in terms of E_2 yields

$$\frac{\Lambda_1 M}{\delta + M}\left(1 - \frac{a(M)}{\mu_S + \alpha_T M}\right) = f(M)E_2,$$

where

$$f(M) = \left[\frac{a(M)\gamma_1 M}{\mu_S + \alpha_T M} + \frac{(\mu_T + \lambda_3 M)\eta M}{\mu_T + \lambda M} + \mu_1\right] g(M) + \frac{a(M)\gamma_2 M}{\mu_S + \alpha_T M} + \mu_2 + \beta M.$$

Let

$$\phi(M) := \frac{(\lambda_1 + \lambda_2)\alpha_T M^2}{h(M)} \cdot \frac{\Lambda_1 M}{\delta + M},$$

where

$$h(M) = \left(\frac{\lambda_1}{\lambda_2} + 1\right)(\gamma_2 M + \beta M + \mu_2)(\mu_S + \alpha_T M)(\mu_T + \lambda M) - (\lambda_1 + \lambda_2)\alpha_T M^3(\gamma_1 g(M) + \gamma_2).$$

Then,

$$E_2 = \phi(M), \quad E_1 = g(M) \cdot \phi(M).$$

Thus, all variables S_T, T_A, E_1, E_2, and B are expressed in terms of M.

Substituting these into the last equilibrium condition (equation for $\dot{M} = 0$), we obtain a nonlinear polynomial:

$$P(M) = M \cdot \left[\sum_{i=0}^{7} X_i M^i\right] = 0.$$

Key coefficients are

$$X_7 = -\alpha_T^2\mu_B\mu_M\,(\lambda_1+\lambda_2+\lambda_3)\,(\beta\eta\lambda_1\lambda_2+\beta\eta\lambda_1\lambda_3+\beta\eta\lambda_2^2+\beta\eta\lambda_2\lambda_3+\beta\gamma_1\lambda_1\lambda_2+\beta\gamma_1\lambda_2^2 \\ +\beta\gamma_1\lambda_2\lambda_3+\beta\gamma_2\lambda_1\lambda_3+\eta\gamma_2\lambda_1\lambda_3+\eta\gamma_2\lambda_2\lambda_3+\gamma_1\gamma_2\lambda_2\lambda_3+\gamma_2^2\lambda_1\lambda_3) < 0,$$

and the constant term (after substitution of $\mathcal{R}_0$)

$$X_0 = \mu_1\mu_2\mu_B\mu_S\mu_T^2(2\lambda_1+\lambda_2)\,(\Lambda_1 q-\Lambda_1\mu_S\epsilon_S p_S-\delta\mu_S\mu_M) = C(\mathcal{R}_0-1),$$

where

$$C = \mu_1\mu_2\mu_B\mu_S\mu_T^2(2\lambda_1+\lambda_2)(\delta\mu_S\mu_M+\epsilon_S p_S\Lambda_1\mu_S).$$

Hence,

$$\text{sign}(X_0) = \text{sign}(\mathcal{R}_0-1).$$

Since $X_7 < 0$, and X_0 changes sign with $\mathcal{R}_0$, we conclude as follows:

- if $\mathcal{R}_0 > 1$, $P(M)$ has at least one positive root; this means that sustainable equilibrium exists.
- If $\mathcal{R}_0 < 1$, the possibility of multiple sustainable equilibria exists (backward bifurcation), subject to coefficient variations.

C. Vector form of the system for center manifold reduction

We rewrite system (2.7) in vector form:

$$\frac{d\mathbf{x}}{dt} = (f_1,\cdots,f_6)^T = \mathbf{f}(\mathbf{x},q), \quad \text{with } \mathbf{x} = (x_1,x_2,x_3,x_4,x_5,x_6)^T,$$

where:

$$\begin{aligned}
\frac{\mathrm{d}\,x_1}{\mathrm{d}\,t} &= \frac{\Lambda_1 x_6}{\delta+x_6}+\gamma_1 x_6 x_3+\gamma_2 x_6 x_4-\alpha_T x_6 x_1-\mu_S x_1,\\
\frac{\mathrm{d}\,x_2}{\mathrm{d}\,t} &= \alpha_T x_6 x_1+\eta x_6 x_3-(\lambda_1+\lambda_2+\lambda_3)x_6 x_2-\mu_T x_2,\\
\frac{\mathrm{d}\,x_3}{\mathrm{d}\,t} &= \lambda_1 x_6 x_2-(\gamma_1+\eta)x_6 x_3-\mu_1 x_3,\\
\frac{\mathrm{d}\,x_4}{\mathrm{d}\,t} &= \lambda_2 x_6 x_2-(\gamma_2+\beta)x_6 x_4-\mu_2 x_4,\\
\frac{\mathrm{d}\,x_5}{\mathrm{d}\,t} &= \lambda_3 x_6 x_2+\beta x_6 x_4-\mu_B x_5,\\
\frac{\mathrm{d}\,x_6}{\mathrm{d}\,t} &= q(x_1+x_2+x_3+x_4+x_5)-\mu_M x_6-\epsilon_S p_S\left(\frac{\Lambda_1 x_6}{\delta+x_6}+\gamma_1 x_6 x_3+\gamma_2 x_6 x_4\right)\\
&\quad -\epsilon_L p_L\lambda_2 x_6 x_2-\epsilon_T p_T(\alpha_T x_6 x_1+\eta x_6 x_3)-\epsilon_A p_A\lambda_1 x_6 x_2-\epsilon_B p_B(\lambda_3 x_6 x_2+\beta x_6 x_4).
\end{aligned}$$

D. eFAST sensitivity indices for state variables

This section provides the extended FAST (eFAST) sensitivity results for the following model state variables: T_A (women undergoing eligibility testing for ablative treatment), E_1 (women receiving

ablative treatment), E_2 (women receiving LLETZ treatment) and B (women undergoing confirmation biopsy).

Each figure shows both first-order ($S1$) and total-order (ST) sensitivity indices for key input parameters.

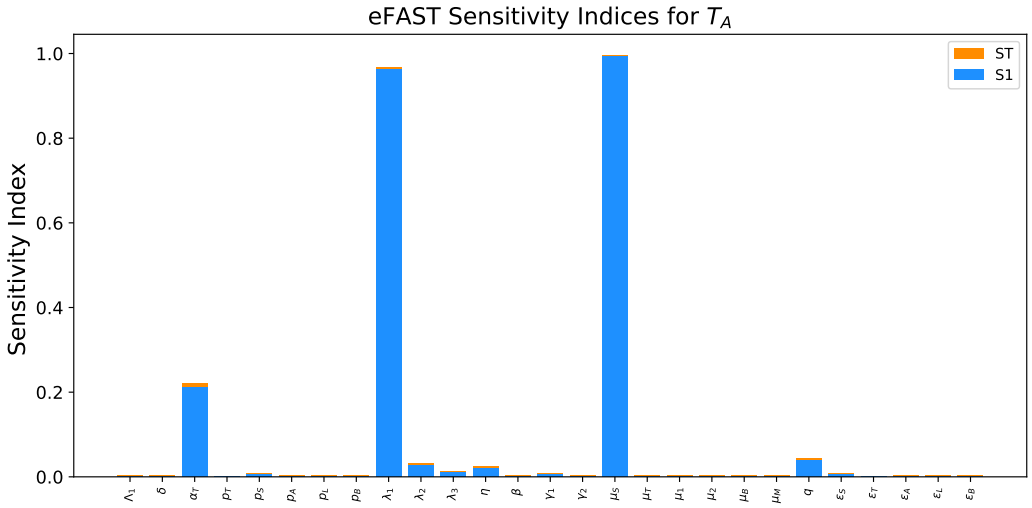

Figure A1. eFAST sensitivity indices for T_A (eligibility testing).

Figure A1 shows that the eligibility testing compartment is driven by a small group of parameters, with markedly different influence patterns. The most influential parameters are the exit rate of screened women μ_S, whose first-order and total-order indices dominate all others and the transition rate λ_1 which governs movement from eligibility testing toward ablative treatment. This indicates that the overall size of the T_A compartment is strongly constrained by the rate at which women leave the screening stage and the distribution of eligible women across treatment pathways. The eligibility transition parameter α_T also exhibits a substantial effect, confirming that the mechanism by which screened women enter the eligibility-testing stage remains structurally important. Finally, the daily patient contribution rate q appears as a fourth, but comparatively smaller, contributor, acting globally on the financial feedback loops that modulate compartment sizes. All other parameters including screening inflow parameters (Λ_1, δ), test and treatment costs, and downstream clinical rates (γ_1, γ_2, η, β), show negligible influence on this compartment. Overall, these results suggest that the variability of T_A is shaped primarily by the balance between exit rate from screening compartment (μ_S) and transitions into and out of the eligibility stage (α_T, λ_1). Policies aiming to regulate or stabilize the eligibility queue should therefore focus on improving retention after screening, strengthening the screening-to-eligibility transition, and managing the flow of patients into treatment rather than modifying cost parameters or upstream detection efforts.

Figure A2 indicates that the ablative treatment compartment is mainly driven by the screening-exit rate μ_S and the return-to-screening rate γ_1, which exhibit the strongest influence. The parameter μ_S affects E_1 indirectly by regulating how many women progress from screening to eligibility testing and ultimately into ablative care. In contrast, γ_1 governs the rate at which successfully treated women leave E_1 and re-enter the screening cycle for follow-up, thereby shaping the long-term size of this compartment through a feedback mechanism. Secondary influences include the daily patient contribution q, the transition rate to ablation λ_1, and the eligibility-test transition parameter α_T. All other parameters have negligible effects, suggesting that once women reach this compartment, its dynamics are largely

insensitive to downstream cost variations. This sensitivity structure highlights that the long-term sustainability of the ablative treatment compartment is shaped more by clinical outcomes and feedback mechanisms than by upstream detection processes. A high value of γ_1 reinforces a cyclical loop in which successfully treated women return to the screening pathway, thereby increasing the number of individuals who may re-enter downstream stages in later periods. This dynamic means that even if the unit cost of ablation is relatively low, the cumulative demand it generates over time may be substantial, particularly in settings where follow-up screening is encouraged or systematically implemented. Conversely, the dominance of μ_S suggests that the rate at which women exit the screening stage critically determines how many ultimately reach ablative care. Improvements in retention or follow-through at the screening level can therefore have a non-negligible downstream impact on the size of E_1. The moderate influence of q, λ_1, and α_T indicates that financial feedback and transition mechanisms still modulate this compartment, but to a lesser degree. Overall, the sensitivity profile underscores that effective management of ablation services requires balancing clinical success (via γ_1) with efficient flow control at the screening and eligibility stages (via μ_S and α_T), in order to prevent excessive long-term demand on treatment capacity.

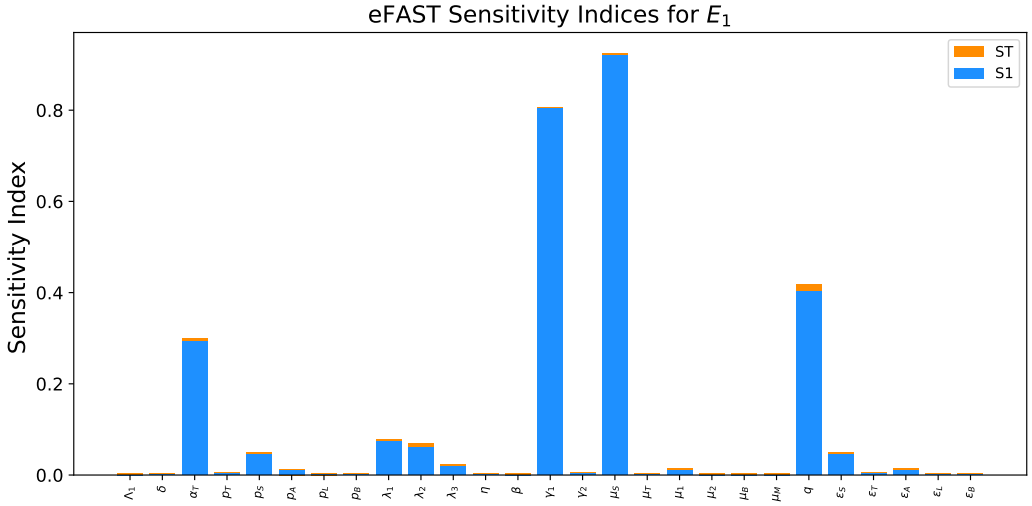

Figure A2. eFAST sensitivity indices for E_1 (ablative treatment).

Figure A3 shows that the LLETZ compartment is now dominated by the screening exit rate μ_S, which exerts the strongest overall influence. This parameter affects E_2 indirectly by regulating how many women progress from screening to eligibility testing and subsequently enter the treatment cascade. Alongside μ_S, the transition rates λ_1 and γ_2 remain highly influential, followed by λ_2 and the daily patient contribution q. Secondary effects arise from the subsidy on eligibility testing (ϵ_T) and the transition-to-eligibility parameter α_T, whereas all other parameters have negligible impact. Altogether, this profile indicates that the flow into E_2 is shaped by both upstream screening dynamics (via μ_S) and the distribution of patients between ablative and LLETZ treatment pathways (via λ_1 and λ_2), as well as by the effectiveness of post-treatment reintegration into screening (via γ_2). Financial factors such as q and ϵ_T also contribute meaningfully to sustaining this compartment. This sensitivity structure suggests that the economic and clinical burden associated with LLETZ depends strongly on how women are filtered through the early stages of care and allocated between competing treatment options. Since LLETZ carries a higher unit cost than ablation, even moderate shifts in transition rates particularly increases in λ_2 relative to λ_1 can significantly elevate cumulative expenditures. The prominence of γ_2

further indicates that successful LLETZ outcomes, while clinically desirable, reinforce the feedback loop back into screening and may thus generate repeated downstream demand. The dominant role of μ_S highlights that upstream screening losses or retention can profoundly modify the number of women reaching advanced treatment stages. Overall, these results show that LLETZ may become a primary driver of escalating costs when its share of treatment allocation increases or when early-stage patient outflow is insufficiently controlled.

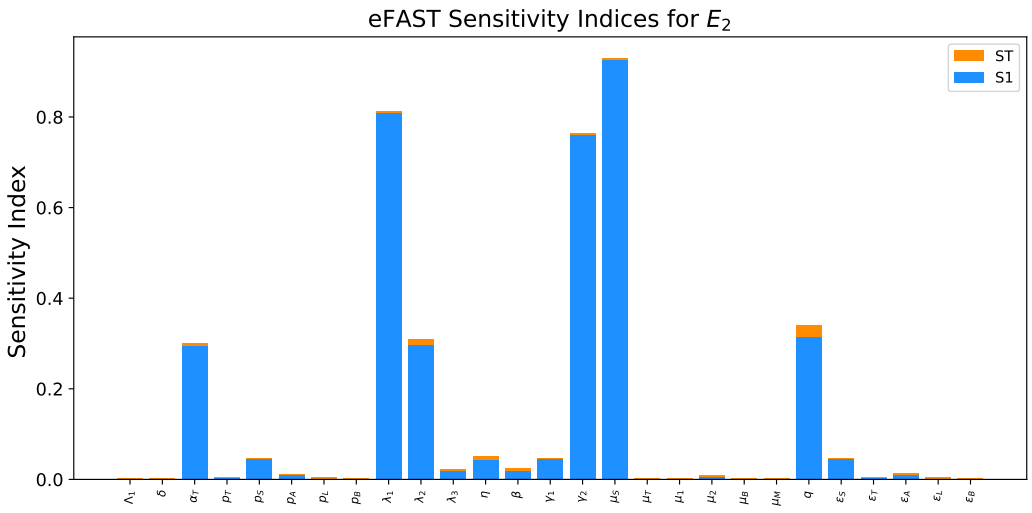

Figure A3. eFAST sensitivity indices for E_2 (LLETZ treatment).

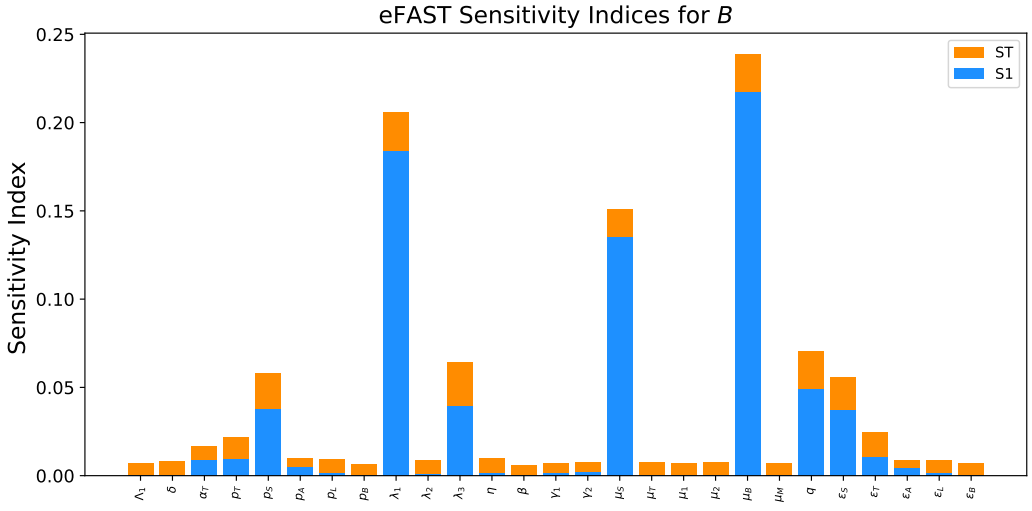

Figure A4. eFAST sensitivity indices for B (biopsy).

Figure A4 reveals that the biopsy compartment is primarily driven by the exit rate μ_B, which exhibits the strongest influence among all parameters. This dominance reflects the fact that the duration patients spend in the biopsy stage is the main factor regulating the overall size of this compartment. The second most influential parameter is the transition rate λ_1, which governs the flow of women routed toward ablative treatment rather than LLETZ; by shaping upstream treatment allocation, λ_1 indirectly determines how many women ultimately require biopsy confirmation. The screening-exit rate μ_S also

plays a significant role, indicating that upstream retention or loss during screening strongly influences how many patients progress through the care cascade to reach the diagnostic stage. Beyond these three parameters, a group of secondary influences persists, including the daily patient contribution q, upstream treatment transition rates (λ_2, λ_3), and cost-related parameters such as p_S and ϵ_S. These factors regulate the overall volume of patients entering the system, the distribution across treatment pathways, and the financial constraints acting on early stages of care.

In sum, the global sensitivity analysis of model (2.7) using eFAST highlights a coherent pattern across all state variables. The dynamics of the screened population (S_T) are most sensitive to the transition toward eligibility testing (α_T), the exit rate in screening compartment (μ_S), and the daily patient contribution (q), showing that early-stage access and continuity of care depend primarily on financial and biological constraints. The treatment account (M) is similarly dominated by α_T, p_S, q, and the costs and subsidies associated with screening (p_S, ϵ_S), indicating that financial sustainability is largely dictated by the balance between inflows from patient contributions and outflows linked to the first diagnostic step. Once women progress to the eligibility compartment (T_A), the critical factors are especially μ_S, λ_1, and α_T, which determine how patients are allocated between ablation and LLETZ. The downstream treatment compartments reflect this distribution: Ablative treatment (E_1) is strongly influenced by the return-to-screening rate γ_1, while LLETZ (E_2) depends on a mix of allocation parameters (λ_1, λ_2) and treatment success (γ_2), with financial contributions maintaining a moderate role. The biopsy compartment (B), though small in size, is heavily shaped by its exit rate (μ_B). Taken together, these results suggest that the economic burden of the system is primarily determined by upstream factors: the probability of testing positive and transitioning to eligibility, the level of patient contributions, and the cost and subsidy structure of the initial HPV test. Downstream parameters, while important for clinical outcomes, play a secondary role in shaping overall expenditures.

AIMS Press